

Reionization of the Inhomogeneous Universe

Jordi Miralda-Escudé^{1,4}, Martin Haehnelt^{2,3}, Martin J. Rees²

¹ Univ. of Pennsylvania, Dept. of Physics and Astronomy

² Institute of Astronomy, University of Cambridge

³ Max-Planck-Institut für Astrophysik, Garching

⁴ Alfred P. Sloan Fellow

ABSTRACT

A model of the density distribution in the intergalactic medium, motivated by that found in numerical simulations, is used to demonstrate the effect of a clumpy IGM and discrete sources on the reionization of the universe. In an inhomogeneous universe reionization occurs outside-in, starting in voids and gradually penetrating into overdense regions. Reionization should not be sudden but gradual, with a continuous rise of the photon mean free path over a fair fraction of the Hubble time as the emissivity increases. We show that a hydrogen Gunn-Peterson trough should be present at $z \simeq 6$ unless the emissivity increases with redshift at $z > 4$. However, the epoch of overlap of cosmological H II regions could have occurred at a higher redshift if sources of low luminosity reionized the IGM; the Gunn-Peterson trough at $z \sim 6$ would then appear because even the most underdense voids have a large enough neutral fraction in ionization equilibrium to be optically thick to Ly α photons. Cosmological H II regions near the epoch of overlap can produce gaps of transmitted flux only if luminous quasars contributed to the reionization, producing large H II regions. Despite the clumpiness of the matter distribution, recombinations do not increase the required emissivity of ionizing photons by a large factor during the reionization of hydrogen because the high density gas is not ionized until a late time. We show that the He II reionization was most likely delayed relative to the hydrogen reionization, but was probably complete by $z \sim 3$ (the redshift where observations are available). The reported large optical depth fluctuations of He II are not necessarily due to an incomplete He II reionization, but can arise from a combination of IGM density fluctuations and variations in the intensity of the He II ionizing background due to luminous QSO's.

Subject headings: cosmology: theory — intergalactic medium — large-scale structure of universe — quasars: absorption lines

1. Introduction

In the standard Big Bang model, the primordial gas becomes neutral at the recombination epoch, at redshift of $z \simeq 1100$. The absence of the hydrogen Gunn-Peterson trough (which would be expected in high redshift objects if hydrogen were neutral) implies that most of the hydrogen in the intergalactic medium (hereafter, IGM) was highly ionized at redshifts $z \lesssim 5$ (Gunn & Peterson 1965; Bahcall & Salpeter 1965; Scheuer 1965; see Schneider, Schmidt, & Gunn 1991; Dey et al. 1998; Weymann et al. 1998; Fernández-Soto, Lanzetta, & Yahil 1999, for the most recent evidence at the highest redshifts). The double ionization of helium may, however, take place later. Four quasars have been observed so far at the He II Ly α wavelength near a redshift $z = 3$ (Jakobsen et al. 1994, 1996; Davidsen, Kriss, & Zheng 1996; Hogan, Anderson, & Rutgers 1997; Anderson et al. 1998; Heap et al. 1999), which show that a large fraction of the flux is absorbed (about 75% over $2.5 \lesssim z \lesssim 3$); in addition, Heap et al. (1999) show that over 98% of the flux is absorbed in Q0302-003 at $z > 3$, except for some individual, well resolved gaps. Reimers et al. (1997) suggested that variations in the ratio of the He II to the H I optical depth provide evidence that the overlap of He III regions was not yet complete at $z \simeq 3$, but this is still controversial (Miralda-Escudé 1998, Anderson et al. 1998; Heap et al. 1999).

The IGM is well known to be highly inhomogeneous, owing to the non-linear collapse of structure. So far, most analytic treatments of the reionization process have only considered the inhomogeneity of the IGM in terms of a clumping factor that increases the effective recombination rate (e.g., Arons & Wingert 1972; Shapiro & Giroux 1987; Madau, Haardt, & Rees 1998). In this paper, we address the effects of inhomogeneity in more detail. We shall argue that another important factor is that reionization should occur gradually over the time interval during which the emissivity increases, and that denser gas will tend to be ionized at a later time than lower density gas. This can result in the ionization of most of the volume of the universe and the overlap of ionized regions, without the need to ionize very dense gas and therefore without the need to greatly increase the number of recombinations owing to the clumpiness of the IGM.

The inhomogeneity of the gas distribution is also of primary importance to understand the absorption spectra of high redshift sources. The mean flux decrement of the photoionized intergalactic medium (or Ly α forest) increases with redshift. Eventually, as the epoch of reionization is approached, the Ly α forest should turn into a series of “clearings”, or “gaps” of transmitted flux appearing through the otherwise completely opaque Gunn-Peterson trough (Meiksin & Madau 1993; Miralda-Escudé 1998), and the number of clearings should decline rapidly with increasing redshift. Quantitative predictions are needed to assess how this transition takes place in detail, depending on the spatial distribution of gas in the IGM

and on the luminosity function and lifetime of the sources of ionizing photons.

In recent years, numerical simulations have led to considerable progress in the understanding of the density distribution and the ionization state of the IGM (Cen et al. 1994; Hernquist et al. 1996; Miralda-Escudé et al. 1996; Zhang, Anninos, & Norman 1995; Zhang et al. 1998). First attempts have also been made to incorporate ionizing sources and to investigate the corresponding evolution of the ionizing background during the epoch of reionization (Gnedin & Ostriker 1997). Here we use this knowledge of the density distribution of the IGM to make a simple model of the way reionization proceeds.

In §2 we define the concept of the global recombination rate, and show how it determines the advance of reionization. In §3 the evolution of the intensity of the background is expressed in terms of the mean-free path, and we discuss the effects that determine the number of gaps of transmitted flux visible in Ly α spectra as the epoch of reionization is approached. In §4 we study the conditions under which QSO's or star-forming galaxies can meet the requirements for reionization, and we discuss the question of the detectability of single H II regions around individual sources in the Ly α spectra. §5 discusses a number of special aspects of helium reionization, and §6 presents our conclusions. Unless otherwise specified, we use the cosmological model $H_0 = 65 \text{ km s}^{-1} \text{ Mpc}^{-1}$, $\Omega_0 = 0.3$, $\Lambda_0 = 0.7$, $\Omega_b h^2 = 0.019$.

2. Reionization of an Inhomogeneous Intergalactic Medium

The first discussion of the process of the reionization of hydrogen in the universe assumed an IGM with uniform density (Arons & Wingert 1972). It was immediately clear that the ionization would not take place homogeneously, but in individual cosmological H II regions growing around the first sources of ionizing photons. The mean free path of ionizing photons in the neutral IGM, λ , is very small [$\lambda = 0.28 (\Omega_b h^2 / 0.02)^{-1} (1+z)^{-3} \text{ Mpc}$ at the threshold frequency, in proper units]. Unless the sources were very numerous and of low luminosity (with a number density as high as λ^{-3}), the thickness of the ionization fronts should be very small compared to the size of the H II regions, and the IGM should be divided into H II regions around every source and neutral regions in between. As the mean emissivity in the universe grows, the H II regions grow in size until they overlap. Two conditions need to be satisfied before the IGM is completely ionized: one photon for each atom in the IGM needs to be emitted, and the mean photon emission rate must exceed the recombination rate so that the hydrogen atoms are photoionized faster than they can recombine. If recombinations are never important, the H II regions will never reach their Strömgren radius before overlapping. If recombinations are important, then the H II regions

will fill an increasing fraction of the IGM as the emissivity rises and the recombination rate is reduced due to the expansion of the universe. In both of these two cases (and assuming that the size of the H II regions is much smaller than the horizon), the model of the homogeneous IGM implies that there is a universal time when the last neutral regions are ionized. The mean free path of the ionizing photons and the intensity of the background increase very abruptly at this time. The reason for this sudden increase is that the universe is still very opaque to ionizing photons when only a small fraction of the atoms remain to be ionized, and then it becomes transparent in the very short time it takes to ionize these last atoms.

Based on this model, the argument has been put forward that there should be a well-defined “redshift of reionization” at which this sudden rise of intensity takes place (e.g., Haiman & Loeb 1998 and references therein). This conclusion is, however, an artifact of considering a model of the IGM with uniform density. Furthermore, even in a homogeneous model, only the initial increase of the ionizing flux will occur on a timescale short compared to the Hubble time. The build-up of the final flux and the decrease of the mean opacity to values of order unity still takes a fair fraction of the Hubble time for any realistic redshift evolution of the emissivity of ionizing photons.

We shall find in this paper that, when studying the problem of how the increasingly dense Ly α forest turns into a Gunn-Peterson trough at high redshift, the assumption of an IGM with homogeneous density leads to a misleading picture of what actually happens. The inhomogeneous IGM must be considered right from the start, and it is then found that reionization must be a gradual process where the intensity of the background increases over a similar timescale as the emissivity of ionizing radiation.

Let us therefore consider the volume-weighted probability distribution of the overdensity in the IGM, $P_V(\Delta)$, where $\Delta = \rho/\bar{\rho}$, ρ is the gas density and $\bar{\rho}$ is the mean density of baryons. A crucial concept in our analysis will be that of the *global* recombination rate. Imagine that all the gas at density $\Delta < \Delta_i$ is ionized, while the higher density gas is neutral. This assumption clearly cannot be exact, because the degree of ionization of gas of fixed density will depend on the local intensity of ionizing photons and the degree of self-shielding; nevertheless, we shall see that it provides a useful approximation to understand how reionization proceeds. Then, the mean number of recombinations per Hubble time that take place for each baryon in the universe is

$$R(\Delta_i) = R_u \int_0^{\Delta_i} d\Delta P_V(\Delta) \Delta^2. \quad (1)$$

Here, R_u is the ratio of the recombination rate for a homogeneous universe to the Hubble constant, given by $R_u(z) = 0.035 [\Omega_b h(1 - 3Y/4)/0.025] (1 + z)^{3/2}/\Omega_0^{1/2}$ for hydrogen

(we use the high redshift approximation $\Omega(z) \simeq 1$, and a recombination coefficient $\alpha = 4 \times 10^{-13} \text{ cm}^3 \text{ sec}^{-1}$, for temperature $T = 10^4 \text{ K}$; the factor $1 - 3Y/4$ is the ratio of electron to baryon density, valid when helium is only once ionized). For $\Omega_0 = 0.3$ and $h = 0.65$, $R_u = 1$ at $z \simeq 6$. We neglect here the effect of the mean variation of the temperature with the density, which can affect the recombination rate due to the temperature dependence of the recombination coefficient, and the presence of collisional ionization. These effects become important only at low redshifts, when halos with a long cooling time for the hot gas are formed.

Now, we consider how reionization should proceed in an inhomogeneous medium as the sources of ionizing photons appear. Most of the sources will be located in high density regions (galaxies), where stars or quasars can form. There is therefore a first phase of reionization where sources must ionize the dense gas in their host halos. This local absorption can simply be subtracted from the emissivity, so that the effective emissivity for reionizing the IGM counts only the emitted photons that are not absorbed in the halo where the source is located. Low luminosity sources may never be able to ionize the surrounding dense gas, and will then not contribute to the reionization. Thus, the period of reionization of the IGM starts when some sources have ionized their host halos and start emitting ionizing photons to the IGM (notice that the emission will then be anisotropic even for intrinsically isotropic sources, because the local absorption in the host halo will generally be anisotropic). The cosmological H II regions will expand fastest along the directions of lowest gas density, both because fewer atoms need to be ionized per unit volume, and because fewer recombinations take place. As a simple example, if the gas density ρ_g is constant along a narrow solid angle from the source (and for isotropic emission), then the distance d reached by the ionization front along different directions at a fixed time is $d \propto \rho_g^{-1/3}$ when recombinations are neglected, and $d \propto \rho_g^{-2/3}$ when the recombination time is short compared to the age of the ionized region.

The end of this period of reionization is reached when the ionized regions start overlapping, and a typical site in the IGM is illuminated by more than one source. Because the ionization fronts advance fastest along regions of low density, the overlap of H II regions will naturally occur first through the lowest density “tunnels” found between sources, and the denser gas with $\Delta > \Delta_i$ will be left in neutral clumps. At the epoch of overlap the photon mean free path will be of the order of the separation between sources (i.e., the size of the H II regions), and thereafter it will continue to increase as the characteristic density Δ_i increases. The dense gas clumps with $\Delta > \Delta_i$ should then be the observed Lyman limit and damped absorption systems. The intensity of the background is limited by the absorption in these systems, until the photon mean free path increases up to the horizon scale. At this last stage, the universe becomes transparent and the intensity of the background is then

controlled by the redshifting of the radiation.

Of course, the assumption that the stage of ionization of the gas is a function of the gas density only is a crude approximation. Some dense clumps will be ionized early if they are close to a luminous source, and the degree of self-shielding depends on the size of the clump in addition to its density. However, we shall see shortly that there is a simple reason why this approximation should still be a useful one.

We will now write an equation governing the reionization of this inhomogeneous IGM. Let $\epsilon(t)$ be the mean volume emissivity, measured in terms of the number of ionizing photons (with energy above 13.6 eV) emitted for each atom in the universe per Hubble time. We define also the ratio of the mean density of ionizing photons present in the cosmic background to the mean density of atoms, n_J . Then we have

$$\epsilon = \frac{dn_J}{H dt} + \frac{dF_M(\Delta_i)}{H dt} + R(\Delta_i) + n_J \phi , \quad (2)$$

where $F_M(\Delta_i)$ is the fraction of mass with density $\Delta < \Delta_i$. The last term includes the losses of ionizing photons due to redshift. The constant ϕ is defined as $\phi \equiv [I_\nu(\nu_T)] [\int_{\nu_T}^\infty d\nu (I_\nu/\nu)]^{-1}$, where I_ν is the background intensity per unit frequency and ν_T is the threshold frequency for ionization. Equation 2 reflects the statement that for every ionizing photon that is emitted, there must be either a photon added to the existing ionizing background, or a new atom being ionized for the first time, or an atom recombining to compensate for the absorption of an ionizing photon, or a photon being redshifted below the ionization edge of hydrogen (we neglect here the presence of helium).

In this paper we shall consider only the limiting case $n_J \ll \epsilon$, which is valid when the mean free path of the ionizing photons, λ_i , is much smaller than the horizon, and provided also that λ_i/c is much smaller than the timescale over which $\epsilon(t)$ increases. These conditions should generally be valid before the universe becomes transparent (unless the sources evolve synchronously over a timescale much shorter than the Hubble time). The terms containing n_J in equation (2) can then be neglected, so

$$\epsilon = dF_M(\Delta_i)/(H dt) + R(\Delta_i) . \quad (3)$$

In this approximation, the background intensity is given by

$$n_J = \epsilon \frac{H \lambda_i}{c} , \quad (4)$$

and depends only on the instantaneous value of the emissivity (and not its history) because all the photons are absorbed shortly after being emitted.

Armed with equation (3), we can now see the reason why the basic approximation in our model (that gas with $\Delta < \Delta_i$ is ionized, and gas with $\Delta > \Delta_i$ is neutral) is reasonable. The crucial fact is that $R(\Delta_i)$ is an increasing function of Δ_i , so that the global recombination rate is always dominated by the ionized gas with densities near Δ_i ; we shall see in §2.2 that this is true for the expected density distribution in the IGM. Initially, when the first sources appear, the term $dF_M(\Delta_i)/(H dt)$ dominates as gas is ionized for the first time. As previously mentioned, even in this regime the gas at low densities is ionized faster than the high density gas. But as the emissivity increases, $R(\Delta_i)$ will become the dominant term at some point, as long as the photon mean free path remains smaller than the horizon (which we know does not occur until $z \simeq 2$). At this point, the balance between the emissivity and the global recombination rate determines the density Δ_i up to which the gas is ionized as the emissivity rises. Most of the gas with $\Delta > \Delta_i$ cannot possibly be ionized, because the recombination rate would then exceed the emissivity and the dense gas would rapidly become neutral. At the same time, most of the gas with $\Delta < \Delta_i$ needs to be ionized, because as we shall see in §3, the mean free path between regions with $\Delta > \Delta_i$ increases rapidly as a function of Δ_i . Therefore, the typical photon emitted to the IGM will spend most of its trajectory in regions with $\Delta \ll \Delta_i$ before reaching a region with $\Delta \sim \Delta_i$ and being absorbed, implying that if low-density regions were not ionized most photons would need to be absorbed there. In reality, the fraction of gas that is ionized will of course vary gradually over a range of densities around Δ_i , and the effect of this gradual variation is what we neglect by approximating it as a sudden transition at density Δ_i .

This approximation is of course much less accurate before the overlap of H II regions, owing to the large fluctuations in the intensity of ionizing radiation. A better model is then obtained by incorporating the new variable Q_i , the fraction of the volume in the IGM occupied by H II regions. In the volume fraction Q_i , some gas is still neutral because of its high density, whereas in the fraction $1 - Q_i$ all the gas is neutral. Again, we can use the approximation that gas with overdensity $\Delta < \Delta_i$ is ionized in the fraction Q_i of the volume, and the higher gas density is neutral. Equation (3) is then modified to

$$\frac{\epsilon}{Q_i} = \frac{F_M}{Q_i} \frac{dQ_i}{H dt} + dF_M(\Delta_i)/(H dt) + R(\Delta_i) . \quad (5)$$

Notice that ϵ/Q_i is simply the emissivity of sources averaged over the fraction Q_i of the volume only. As before, there is a first epoch where the two terms involving the variation of Q_i and F_M are dominant, and at some point recombinations start dominating globally to balance the emission. If Q_i is still less than unity at this point, we can justify the use of equation (1) for $R(\Delta_i)$ in the following way. In every H II region around individual sources, the radiation along every direction ionizes gas up to a point of high enough density where atoms recombine at the same rate at which the photons are arriving. If $R(\Delta_i)$ is dominated

by the highest densities close to Δ_i , most of the photons are absorbed in a dense region at the end of every beam. Once recombination dominates, these regions should have a typical density Δ_i which is still determined by a balance between the global rates of recombination and emission. There should of course be some gas with $\Delta > \Delta_i$ that is ionized in the clumps close to the luminous sources, but again the majority of photons will be absorbed at densities near Δ_i , where most of the gas clumps become self-shielding at a distance from the source equal to the mean radius of the H II region.

Equation 5 does not determine how Δ_i will increase with ϵ before Q_i reaches unity, because only one equation is provided for the two independent variables Q_i and Δ_i once $\epsilon(t)$ and $F_M(\Delta_i)$ are known. The relative growth of Q_i and Δ_i should depend on the luminosity function and spatial distribution of the sources. When the sources are very numerous, every void can be ionized by sources located at the edges of the void, and the overlap of ionized regions can occur through the thin walls separating voids, so Q_i approaches unity when Δ_i is the characteristic overdensity of these thin walls, $\Delta_i \sim 1$. For rare and luminous sources, the value of Δ_i must be higher before Q_i can be close to unity, so that the mean free path between the neutral clumps with $\Delta > \Delta_i$ is equal to the mean separation between sources near the epoch of overlap. The early stages of reionization are characterized by the growth of Q_i , while Δ_i essentially determines the photon mean free path (which is of order the size of the H II regions before the overlap).

The end of reionization can be precisely defined as the moment when $Q_i = 1$. In other words, after this moment there is no region in the IGM with low density ($\Delta \lesssim 1$) which is not ionized. A word on what is meant by gradual reionization may be useful here. We note that Q_i should reach unity rather fast at some universal redshift, because $1 - Q_i$ will drop roughly exponentially with the mean number of sources seen from a random point, which is proportional to the cube of the mean free path. This implies an almost discontinuous change in the term $\frac{dQ_i}{H dt}$ in equation 5. However, the terms $dF_M(\Delta_i)/(H dt) + R(\Delta_i)$ guarantee that Δ_i , and therefore λ_i and n_J , will not have a sudden increase at this epoch. Gradual reionization means that the logarithmic derivative $dn_J/(n_J H dt)$ will not have a sharply peaked maximum over a very short time interval ($t \ll H^{-1}$), but instead the increase of n_J will take place over \sim a Hubble time.

2.1. The Gas Density Distribution

To examine more quantitatively the effects discussed above, we shall use a model of the gas density distribution in the IGM based on the results obtained from hydrodynamic numerical simulations, which were found to be in good agreement with observations of the

distribution of the transmitted flux in the Ly α forest (Rauch et al. 1997). Here, we obtain a simple analytical fit to the numerical results of the density distribution in the IGM at different redshifts.

The formula we use to fit the result of numerical simulations is motivated by a simple approximation of the evolution of the density in voids. In the limit of low densities, we assume the gas in voids to be expanding at a constant velocity, as should be the case if tidal forces are negligible. Then, the proper density in the void decreases as $\Delta a^{-3} \propto t^{-3} \propto a^{-9/2}$, so $\Delta \propto a^{-3/2}$ (where we assume $\Omega(z) \simeq 1$). Assuming that Δ starts decreasing according to this law when the linear overdensity δ reaches a fixed critical value, and using $\delta \propto a$, we obtain $\Delta \propto (-\delta)^{-3/2}$. The linear density δ is assumed to be smoothed on the Jeans length of the photoionized gas. For Gaussian initial conditions, where $P_V(\delta) \propto \exp[-\delta^2/(2\sigma^2)]$ (with σ being the rms density fluctuation), this yields $P_V(\Delta) \propto \exp(-C\Delta^{-4/3}) \Delta^{-8/3} d\Delta$, where C is a constant. We shall use the following fitting formula, which approaches this limit for $\Delta \ll 1$, and is also applicable in the linear regime when $|\Delta - 1| \ll 1$,

$$P_V(\Delta) d\Delta = A \exp \left[-\frac{(\Delta^{-2/3} - C_0)^2}{2(2\delta_0/3)^2} \right] \Delta^{-\beta} d\Delta. \quad (6)$$

When $\delta_0 \ll 1$ and $C_0 = 1$, the distribution approaches a Gaussian in $\Delta - 1$ with dispersion δ_0 . When $\delta_0 \gg 1$, the distribution goes to the previous approximation for voids, with the peak at a density $\Delta \sim \delta_0^{-3/2}$. Thus, if the median density in voids evolves as $\Delta \propto a^{-3/2}$, then δ_0 should grow proportionally to a both in the linear and the highly non-linear regime. At $\Delta \gg 1$ (and for $\delta_0 \gg 1$), the distribution is a power-law, corresponding to power-law density profiles $\Delta \propto r^{-3/(\beta-1)}$ in collapsed objects (where r is the radius).

We show in Figure 1 the gas density distribution of the L10 simulation described in Miralda-Escudé et al. (1996), together with the fits obtained to equation (6), at the three redshifts $z = 2, 3$ and 4 . The two functions shown at each redshift, for the simulations and the result of the fit, are $\Delta P_V(\Delta)$ and $\Delta^2 P_V(\Delta)$, which are the volume-weighted and mass-weighted probability density of Δ per unit $\log \Delta$, respectively. This density distribution was previously shown in Figure 7 of Rauch et al. (1997) at $z = 2$ only, together with the result from a simulation by Hernquist et al. (1996). As seen in that paper, the density distribution in these two simulations is very similar, since they used models with very similar power spectra. The density distribution should depend mostly on a single parameter, the amplitude of the initial density fluctuations smoothed on the Jeans scale of the photoionized gas. Table 1 gives the values of the four parameters of the fits at each redshift. The parameter δ_0 is indeed approximately proportional to the scale factor.

We have extrapolated the density distribution to higher redshifts by using

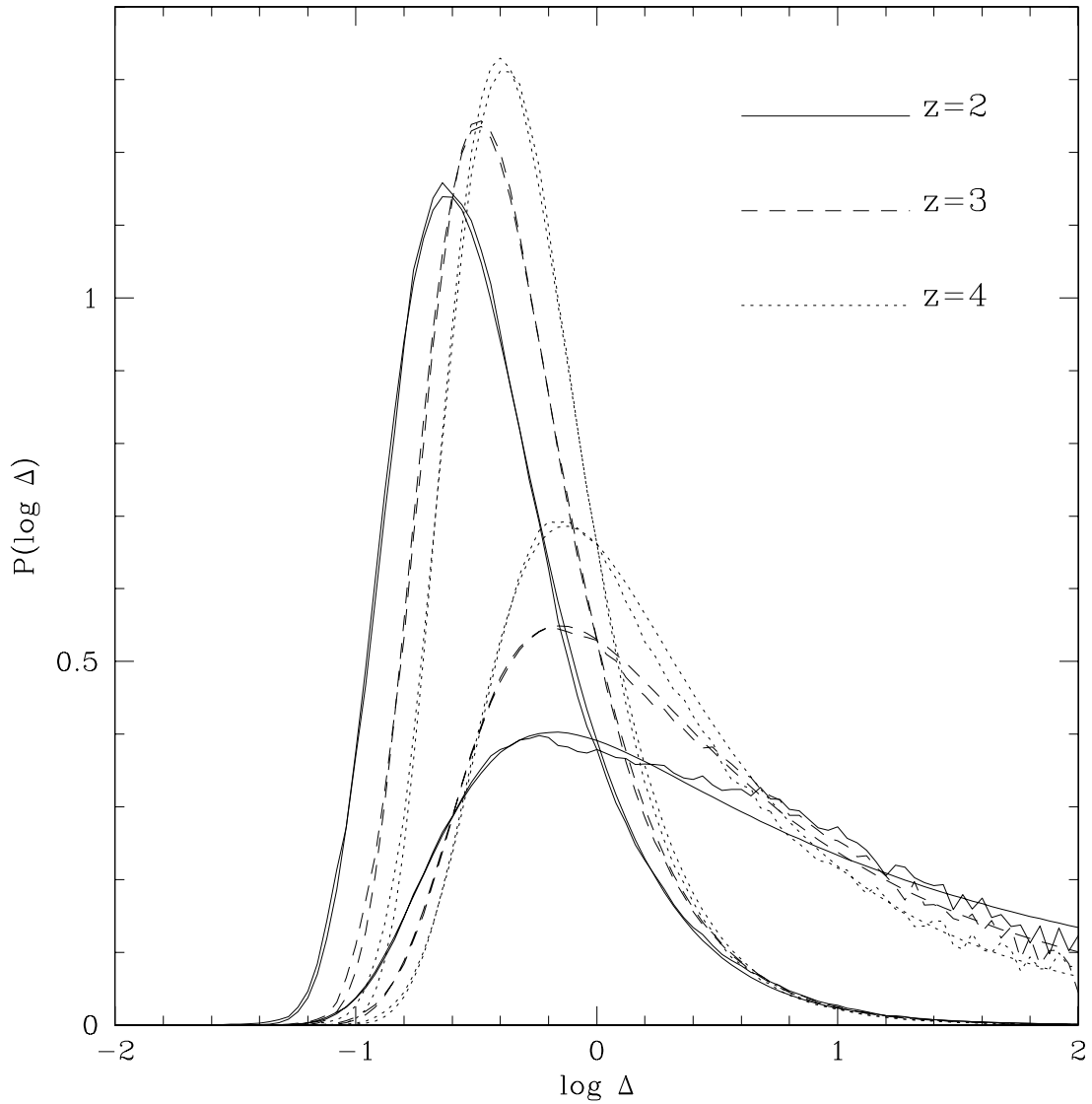


Fig. 1.— Mass and volume-weighted differential density distribution of the IGM, at the three indicated redshifts. The lines with noise are from the numerical simulation in MCOR, and the smooth lines are the fit we have obtained with the analytical model in equation (6).

$\delta_0 = 7.61/(1+z)$, which reproduces the fits in Table 1 to better than 1%. The change of β with redshift is more uncertain (the form of the high-density tail of the distribution in the simulations may also be affected by the resolution); we use $\beta = 2.5$ at $z = 6$, corresponding to an isothermal slope for high density halos. The parameters A and C_0 are then fixed by requiring the total volume and mass to be normalized to unity.

We note here the possibility that a significant fraction of all baryons is contained in small halos with virial temperatures $\sim 10^4$ K, which collapsed to high densities before reionization, when the Jeans mass was very small (e.g., Abel & Mo 1998). These halos (which would not have been resolved in the simulations used for Figure 1) could survive for a long time after reionization occurs if neither star formation nor tidal and ram-pressure stripping due to mergers into larger structures are able to destroy them. In this case, the density distribution would be wider than in our model at high redshift, with a larger fraction of the baryons at very high densities.

2.2. The Global Recombination Rate

In Figures 2(a,b,c), the solid and dotted lines show the cumulative probability distribution of the gas density weighted by mass and volume, respectively, at redshifts $z = 2, 3, 4$. These are obtained from equation (6), with the fit parameters in Table 1. Figure 2d shows the same cumulative distributions obtained at $z = 6$, according to the prescription described for choosing the parameters in equation (6); the values of these parameters at $z = 6$ are also given in Table 1. The dashed line shows the ratio R/R_u as obtained from equation (1).

The model used in equation (1) sets the ionized fraction to unity for $\Delta < \Delta_i$, and to zero for $\Delta > \Delta_i$. Clearly, the change in the mean ionization with Δ should in reality be more gradual. To test the sensitivity of the model to this assumption, we use also an alternative formula for the global recombination rate based on ionization equilibrium with a constant background intensity (notice that the change of the ionized fraction with

Table 1

Redshift	A	δ_0	β	C_0
2	0.406	2.54	2.23	0.558
3	0.558	1.89	2.35	0.599
4	0.711	1.53	2.48	0.611
6	0.864	1.09	2.50	0.880

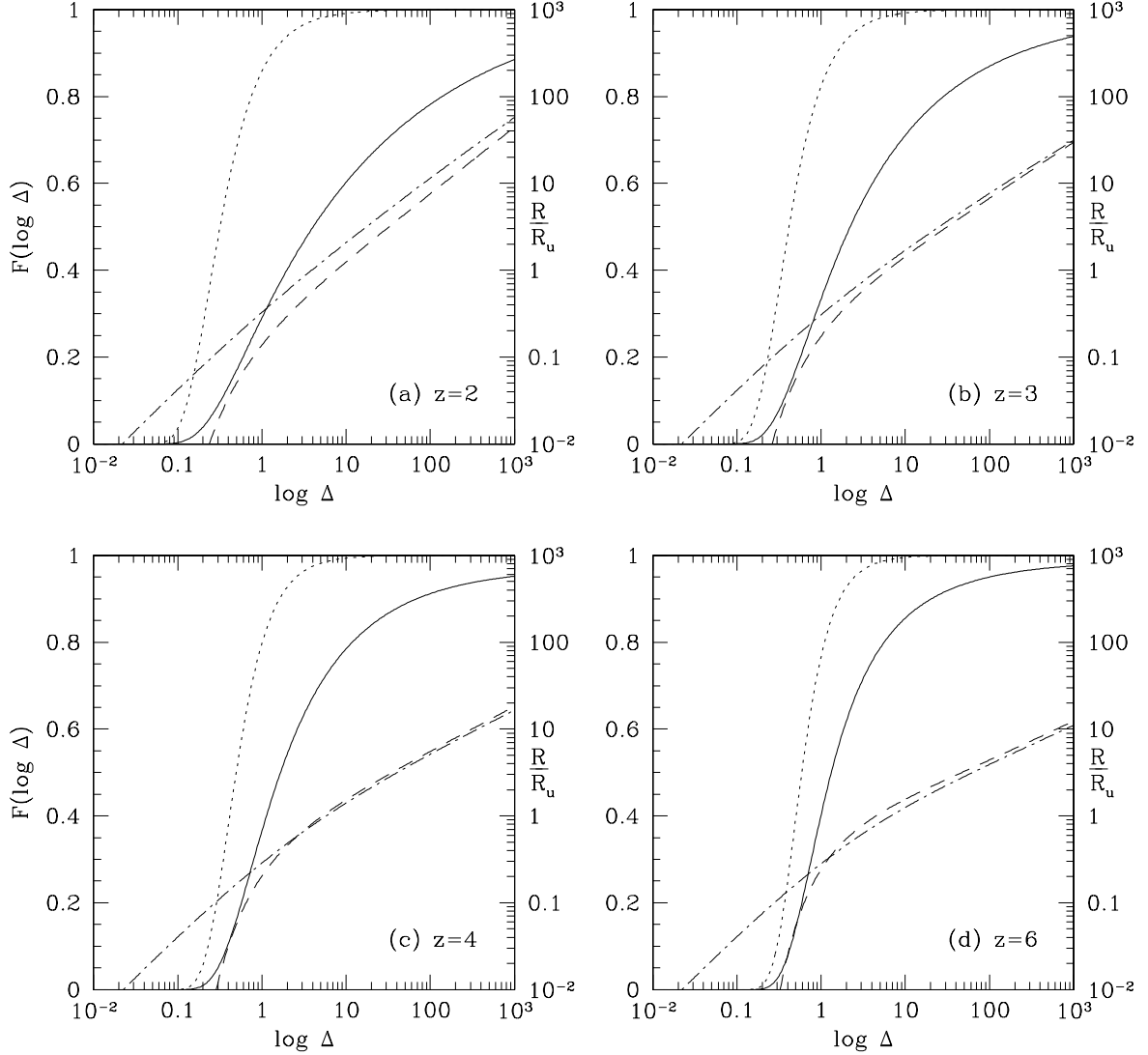


Fig. 2.— Solid and dotted lines are the cumulative density distribution weighted by mass and volume, respectively. The dashed line gives the global recombination rate R when all the gas is assumed to be neutral at overdensities greater than Δ , and ionized at lower overdensities. The dash-dot line is the global recombination rate when ionization equilibrium with a uniform ionizing background is assumed, with the neutral fraction being one half at overdensity Δ . The values of R_u at the redshifts of the four panels, $z = 2, 3, 4, 6$, are $R_u = 0.32, 0.50, 0.71, 1.18$ for hydrogen, and $R_u = 1.89, 2.98, 4.19, 6.99$ for helium (a gas temperature of 10^4 K has been assumed).

density should be steepened by self-shielding effects, and widened by fluctuations in the background intensity and a dispersion in the size of the clumps). The ionized fraction x is then given by $R_u x^2 \Delta^2 = \Gamma \Delta (1 - x)$, where Γ is the photoionization rate, and collisional ionization is neglected. Defining Δ_i as the overdensity where $x = 1/2$ gives $\Delta_i = 2\Gamma/R_u$, and $x = \Delta_i/(4\Delta) [(1 + 8\Delta/\Delta_i)^{1/2} - 1]$, and the global recombination rate is given by $R(\Delta_i) = R_u \int_0^\infty d\Delta P_V(\Delta) x^2 \Delta^2$. This is shown as the dash-dot line in Figure 2. The result is very similar to the case of the sudden change of the ionized fraction, except for $\Delta_i \lesssim 1$ (where the model is not relevant anyway because even at the earliest stages of reionization, with $Q_i \ll 1$, Δ_i should be of order unity or larger).

As long as $P_V(\Delta)$ is less steep than Δ^{-3} at large Δ , $R(\Delta_i)$ should increase monotonically with Δ_i , as seen in Figure 2. This property of the global recombination rate is the main reason why high-density regions should generally be ionized at a later stage than low-density regions when there is a balance between global recombination and emissivity. If low-mass, dense halos formed before reionization and not resolved in the simulation we use were present, then the wider density distribution implied would cause a more rapidly increasing global recombination rate with Δ_i .

The late ionization of the high-density gas implies that the clumpiness of the IGM does not necessarily increase the number of photons required to complete reionization. As an example, if overlap occurs at $z = 6$ and with $\Delta_i = 3$, only about 70% of the baryons need to have been ionized, but 95% of the volume is ionized (Fig. 2d). The dashed curves also show that $R/R_u = 1$ at $\Delta_i \sim 3$, so clumpiness in this case does not increase the net number of recombinations, and actually makes reionization *easier* by reducing the fraction of baryons that need to be ionized. In fact, if additional gas is in small-scale, high-density halos not resolved in the simulations, the required number of photons to complete reionization should be further decreased. Since $R_u \simeq 1$ at $z = 6$, only about one ionizing photon per baryon needs to be emitted to complete reionization. A low value of Δ_i at the epoch of overlap requires that the sources are numerous; reionization by more luminous sources would imply a higher Δ_i , and therefore a greater number of recombinations.

3. The Lyman Alpha Flux Decrement

We now address the question of the flux decrement that should be observed to the blue of the Ly α wavelength, as the redshift increases toward the epoch of reionization. The optical depth of a uniform, completely neutral IGM, τ_0 , is extremely large,

$$\tau_0 = 2.6 \times 10^5 [\Omega_b h(1 - Y)/0.03] [H_0(1 + z)^{3/2}/H(z)] [(1 + z)/7]^{3/2}. \quad (7)$$

Because of this, a small neutral fraction is sufficient to yield a high enough optical depth to make the transmitted flux undetectable, so the Ly α spectrum might already be completely blocked at redshifts lower than the epoch of overlap.

3.1. The mean free path of the ionizing photons

In the simple model where all the gas at densities $\Delta > \Delta_i$ is still neutral, and all the gas at lower densities is ionized, a photon is absorbed whenever it enters a region with $\Delta > \Delta_i$, assuming that these regions are sufficiently large to be optically thick. The mean free path λ_i is then simply the mean length of regions with $\Delta < \Delta_i$ along random lines of sight. Of course, in reality there should be a gradual change of ionization, and differences in the geometrical shape of the structures will cause varying degrees of self-shielding at a given gas density, so photons will be absorbed over a range of densities. Nevertheless, since most of the recombinations take place at densities near Δ_i , most of the photons will be absorbed by gas near this density. The spacing between successive contours at Δ_i should then provide a reasonable estimate of the mean free path. Notice that we assume that λ_i is larger than the mean free path for the case of a uniform IGM, $\lambda_u = [n_a \bar{\sigma} (1 - F_M)]^{-1}$, where n_a is the density of atoms, $\bar{\sigma}$ is a frequency-averaged photoionization cross section, and F_M is the fraction of mass in gas with $\Delta < \Delta_i$. If $\lambda_u > \lambda_i$, then the neutral clumps are optically thin and the mean free path is close to λ_u independently of the density structure of the IGM. We also emphasize that λ_i is the mean free path only for photons that escape into the IGM. Sources of photons will generally appear in regions of high density, and some fraction of the photons will be absorbed locally; these photons are not counted in the mean emissivity ϵ in equations (2) and (3).

Here, we shall use a very simple model for the mean free path of ionizing photons. We assume

$$\lambda_i = \lambda_0 [1 - F_V(\Delta_i)]^{-2/3}, \quad (8)$$

where $F_V(\Delta_i)$ is the fraction of the volume with $\Delta < \Delta_i$. In the limit of high densities, when $1 - F_V \ll 1$, this is valid for any population of absorbers where the number density and shape of isolated density contours remains constant as Δ_i is varied: the fraction of volume filled by the high density regions is $1 - F_V$, so their size is proportional to $(1 - F_V)^{1/3}$, and the separation between them along a random line of sight is proportional to $(1 - F_V)^{-2/3}$. The shape of the absorbers in large-scale structure theories is actually highly complex, with structures varying from ellipsoidal to filamentary to sheet-like as Δ_i is reduced. However, we have found that the proportionality $\lambda_i \propto (1 - F_V)^{-2/3}$ is still approximately obeyed in the results of numerical simulations with photoionized gas dynamics, for $\Delta_i \gtrsim 1$ (see e.g.,

Fig. 3 of MCOR).

In this paper, we shall use the scale $\lambda_0 H = 60 \text{ km s}^{-1}$, which reproduces the scales of the Ly α forest structures in the simulation of the cold dark matter model with a cosmological constant at redshift $z = 3$ in MCOR (designated as L10 simulation in that paper). Although the scale λ_0 should vary with redshift and with the cosmological model, the quantity $\lambda_0 H$ stays roughly constant in this simulation. In fact, $\lambda_0 H$ is basically determined by the Jeans length of photoionized gas at high redshift, when the amplitude of density fluctuations reaches non-linearity at the Jeans scale; it should then increase at lower redshifts as structures collapse on larger scales. This increase might not be fully reflected in numerical simulations like those in MCOR owing to the small size of the simulated box.

3.2. Optical depth of the ionized IGM

Our next step is to compute the optical depth to Ly α scattering through the ionized IGM, τ_i , in a region of density Δ . This is equal to $\tau_0 \Delta$ (eq. 7), times the neutral fraction, which we assume to be in ionization equilibrium. For a constant gas temperature, this optical depth is

$$\tau_i = \tau_0 \frac{\alpha}{\bar{\sigma} c n_J} \frac{\Delta^2}{f_J}, \quad (9)$$

where α is the recombination coefficient (we assume full ionization and neglect the effect of double helium ionization on the electron density), $\bar{\sigma}$ is the frequency-averaged photoionization cross section, and we have defined f_J to be the ratio of the local photon density of the ionizing background at a given point in the IGM to the mean photon density n_J , given by equation (4). The local intensity fluctuates due to the discreteness of the sources that can illuminate a given point. Before the H II regions around individual sources overlap, the intensity fluctuations are of course very large, but they are rapidly reduced after the mean free path increases to values larger than the typical separation between neighboring sources (Zuo 1992; Zuo & Phinney 1993).

Substituting equations (4) and (8) into (9), we obtain for the optical depth of an ionized region,

$$\tau_i = \tau_0 \frac{\alpha}{\bar{\sigma} c} \frac{c}{H \lambda_0} (1 - F_V)^{2/3} \frac{\Delta^2}{\epsilon f_J}. \quad (10)$$

Notice that F_V depends on Δ_i , determining the maximum densities that are ionized, while Δ is the density in the region yielding an optical depth τ_i . The mean emissivity ϵ can be obtained from equation (3). The term $dF_M/(H dt)$ in equation (3) obviously depends on the model for the emitting sources, but if the sources do not evolve on timescales

much shorter than the Hubble time, then $dF_M/(H dt) \sim 1$. Here we shall simply use the expression $\epsilon = 1 + R$; the important point is that $\epsilon = R$ when recombination dominates, and $\epsilon \sim 1$ when most of the baryons are being ionized if recombinations are not important. Thus, we have

$$\tau_i = 1.73 \frac{\Omega_b h(1 - Y)}{0.03} \frac{H_0(1 + z)^{3/2}}{H(z)} \left(\frac{1 + z}{7} \right)^{3/2} \frac{c}{H\lambda_0} \frac{(1 - F_V)^{2/3}}{1 + R} \frac{\Delta^2}{f_J} \equiv \tau_u \frac{\Delta^2}{f_J}. \quad (11)$$

We have used a value $\bar{\sigma} = 2 \times 10^{-18} \text{ cm}^{-2}$, which should be approximately valid for the spectra emitted by quasars or star-forming galaxies. This equation can also be expressed in terms of the recombination rate for a uniform IGM, R_u ,

$$\tau_u = \frac{\tau_0}{\bar{\sigma} n_e \lambda_0} \frac{(1 - F_V)^{2/3}}{(1 + R)/R_u} = 1.14 \frac{c}{H\lambda_0} \frac{(1 - F_V)^{2/3}}{(1 + R)/R_u}, \quad (12)$$

where n_e is the electron density.

The value of τ_u as a function of Δ_i is shown in Figure 3, at redshifts $z = 2, 3$ and 4 . We have used $c/(H\lambda_0) = 5000$, and the cosmological model mentioned in the introduction. As Δ_i increases, the larger mean free path of the photons results in an increasing intensity of the ionizing background, and that decreases the optical depth of the ionized regions. The variation of $\tau_u(\Delta_i)$ with redshift can be understood as follows: ignoring the variation of the density distribution F_V with redshift, and for large Δ_i , we have $R \gg 1$, and τ_u is independent of redshift from equation (12). For small Δ_i , τ_u increases with redshift since $R \ll 1$.

If the IGM were homogeneous, the mean flux decrement due to Ly α scattering would simply be $e^{-\tau_u}$, but for the real IGM the dependence of the flux decrement on τ_u is of course more complicated. The mean flux decrement of the Ly α forest obtained from the simulation in MCOR is shown as a function of τ_u in Figure 4, at redshifts $z = 2, 3, 4$. These curves were computed directly from the simulation, and therefore include the effects of thermal broadening and peculiar velocity; they were shown also in Fig. 19 in MCOR (although with a different scaling in the horizontal axis). Each curve starts at the point where the flux decrement is equal to the observed value (see Press, Rybicki, & Schneider 1993; Rauch et al. 1997). Therefore, in the MCOR model, if all the baryons were spread out uniformly in the IGM keeping the intensity of the ionizing background fixed, the optical depth to Ly α scattering would be $\tau_u = (0.3, 1, 4)$ at $z = (2, 3, 4)$. The curves show how the flux decrement would increase at a fixed redshift if the intensity of the background was reduced, increasing the value of τ_u . At fixed τ_u , the flux decrement increases slightly with redshift. The reason is that voids become more underdense with time, and therefore the amount of flux that is transmitted through the most underdense regions for high τ_u decreases.

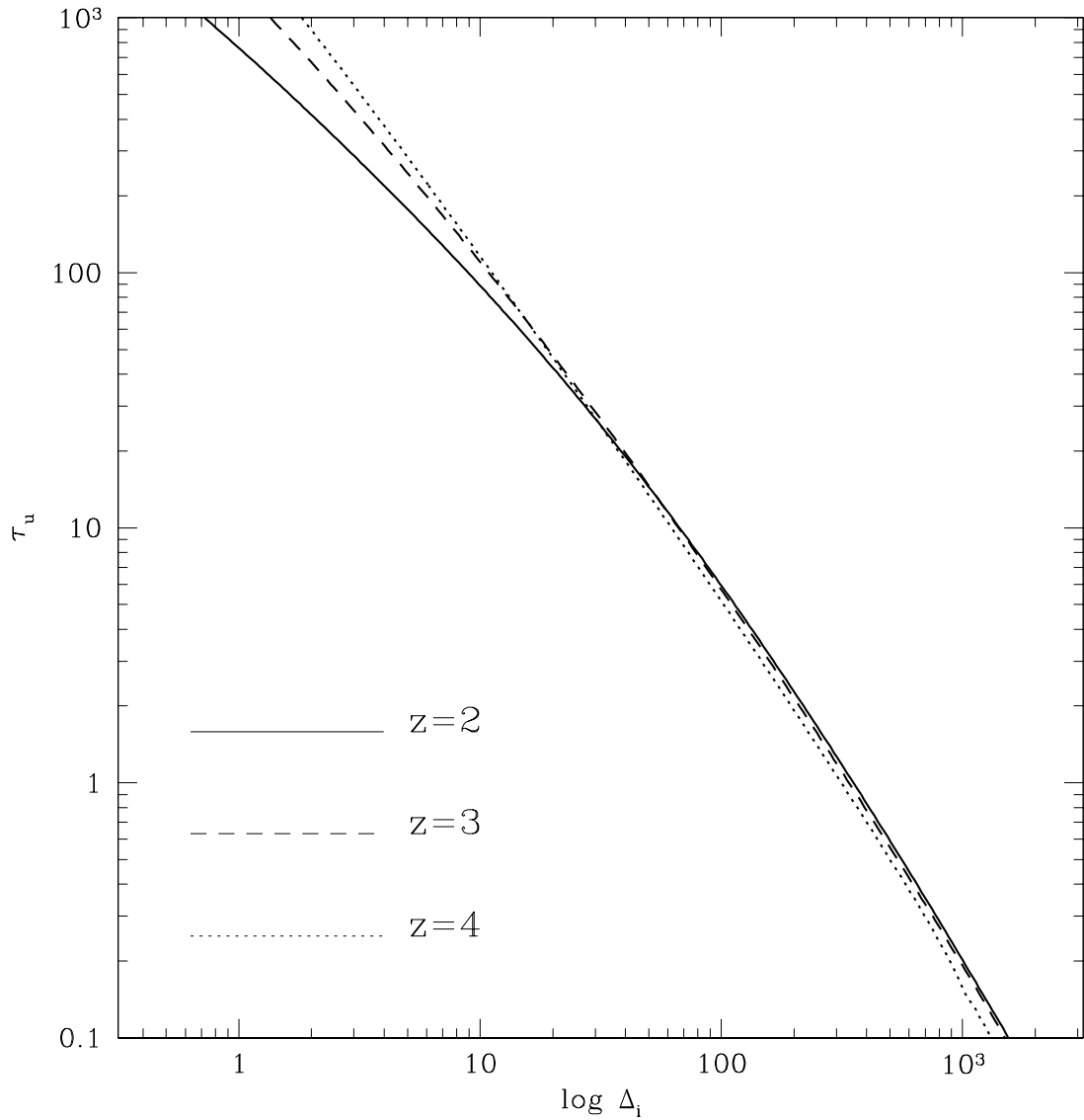


Fig. 3.— Optical depth τ_u that a uniform IGM would yield for the intensity of the ionizing background derived when the emissivity and the mean free path are given by the global recombination rate and our mean free path model, as a function of the overdensity to which the inhomogeneous IGM is ionized.

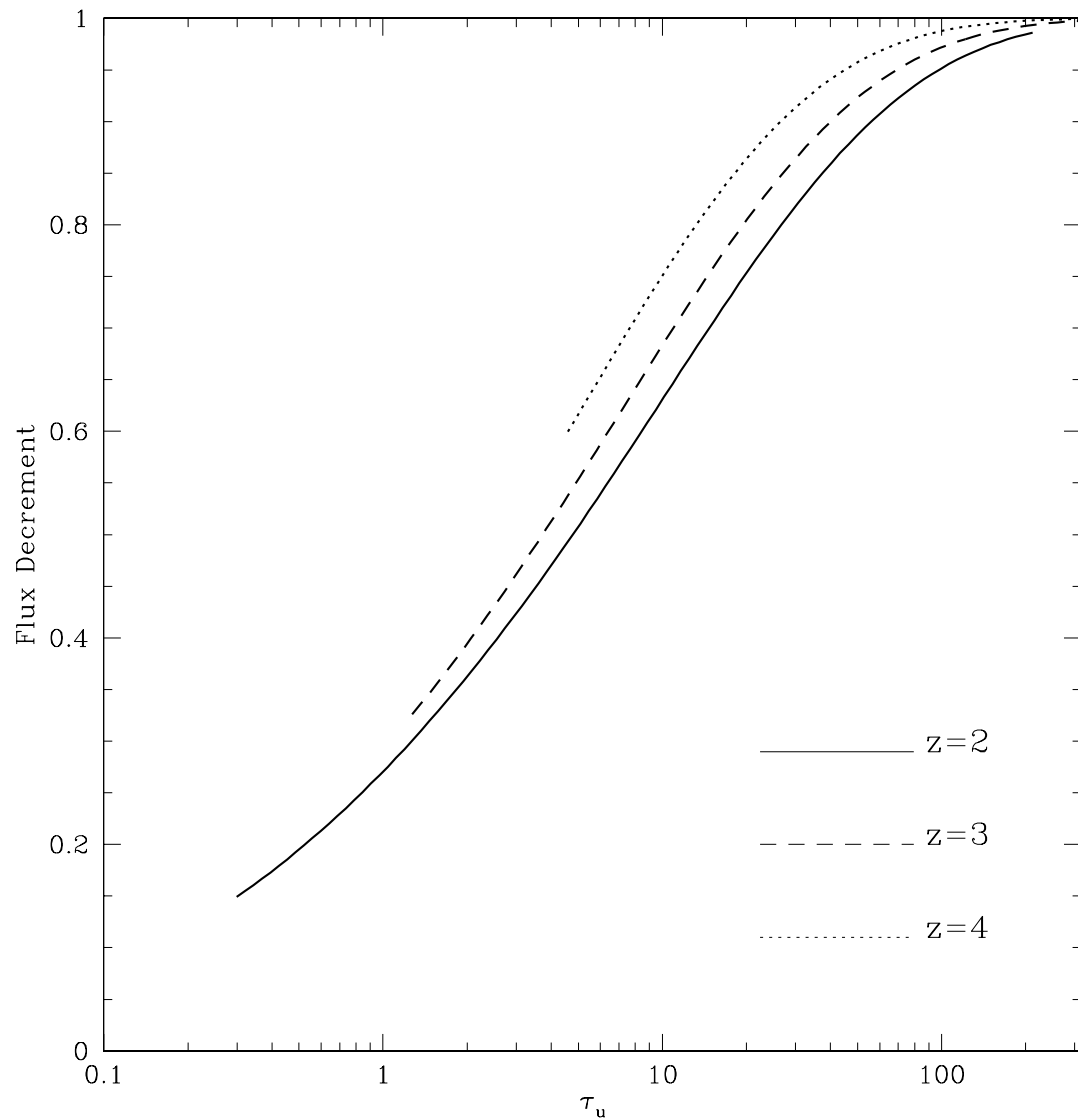


Fig. 4.— Mean flux decrement as a function of the optical depth that a uniform IGM with the same mean density and intensity of the ionizing background would have.

3.3. What is the redshift where the Gunn-Peterson trough is reached?

As sources at progressively higher redshift are being discovered, one of the most interesting questions that arise is: what is the redshift at which a complete Gunn-Peterson trough will first appear? It is often assumed that the Gunn-Peterson trough should appear when the epoch of reionization is reached. However, a small neutral fraction suffices to make the IGM opaque to Ly α photons everywhere, given the enormous value of the optical depth for a neutral medium (eq. 7). In ionization equilibrium with a uniform background, the most underdense voids will have the lowest optical depths. For the gas density distribution used in §2, the lowest densities are $\Delta \simeq 0.1$ at $z = 2$ and $\Delta \simeq 0.25$ at $z = 6$. Since the optical depth is proportional to Δ^2 , the transmitted flux ought to decrease very rapidly to negligible levels when τ_u reaches the inverse square of the lowest underdensities in voids, as the curves in Figure 4 show (the peculiar velocity effect in voids helps to allow for some transmitted flux at slightly higher values of τ_u).

Figure 5 shows the same flux decrement as in Figure 4, plotted as a function of Δ_i . The large filled squares are the values of the observed transmitted flux, according to Rauch et al. (1997). The figure therefore provides a prediction for Δ_i as a function of redshift, given our assumed model for the density distribution: the gas in the Lyman limit systems at column densities $\sim 10^{18} \text{ cm}^{-2}$, where the transition from ionized to neutral gas takes place due to self-shielding, should have typical overdensities of order $\Delta_i \sim (700, 300, 100)$ at $z = (2, 3, 4)$. Notice, however, that the approximation of neglecting redshift effects in equation (2) is starting to fail at $z = 2$, so Δ_i should be somewhat underestimated.

It is clear from Figure 5 that, if the trend of decreasing Δ_i with redshift continues at $z > 4$, then the Gunn-Peterson trough should appear at $z \simeq 6$. There are two main reasons for the increase of the flux decrement with redshift. The most important is the decrease of the density Δ_i to which the universe is ionized. The second one is that the flux decrement increases for fixed Δ_i owing to the lower underdensities of voids at high redshift; thus, at $z \simeq 6$ the transmitted flux should drop to 1% at $\Delta_i \simeq 15$.

Figures 2(a,b,c) show that the global recombination rate corresponding to the densities Δ_i of Lyman limit systems mentioned above, at $z = (2, 3, 4)$, are $R/R_u = (40, 15, 6)$, corresponding to an emissivity of $\epsilon = R = (14, 8.1, 4.3)$ photons per baryon per Hubble time. If the trend of decreasing emissivity with redshift continues, clearly the Gunn-Peterson trough will be reached at $z \simeq 6$. In fact, in order to have more than a few percent of transmitted flux at $z = 6$, according to Figures 5 and 2d, we need $\Delta_i \gtrsim 20$ and $\epsilon > 2.5$. Since we defined ϵ as the number of photons emitted per Hubble time, then as long as the emissivity per physical time is not larger at $z = 6$ compared to $z = 4$, the transmitted flux at $z = 6$ should be less than $\sim 3\%$. We emphasize that the reason is not because the epoch

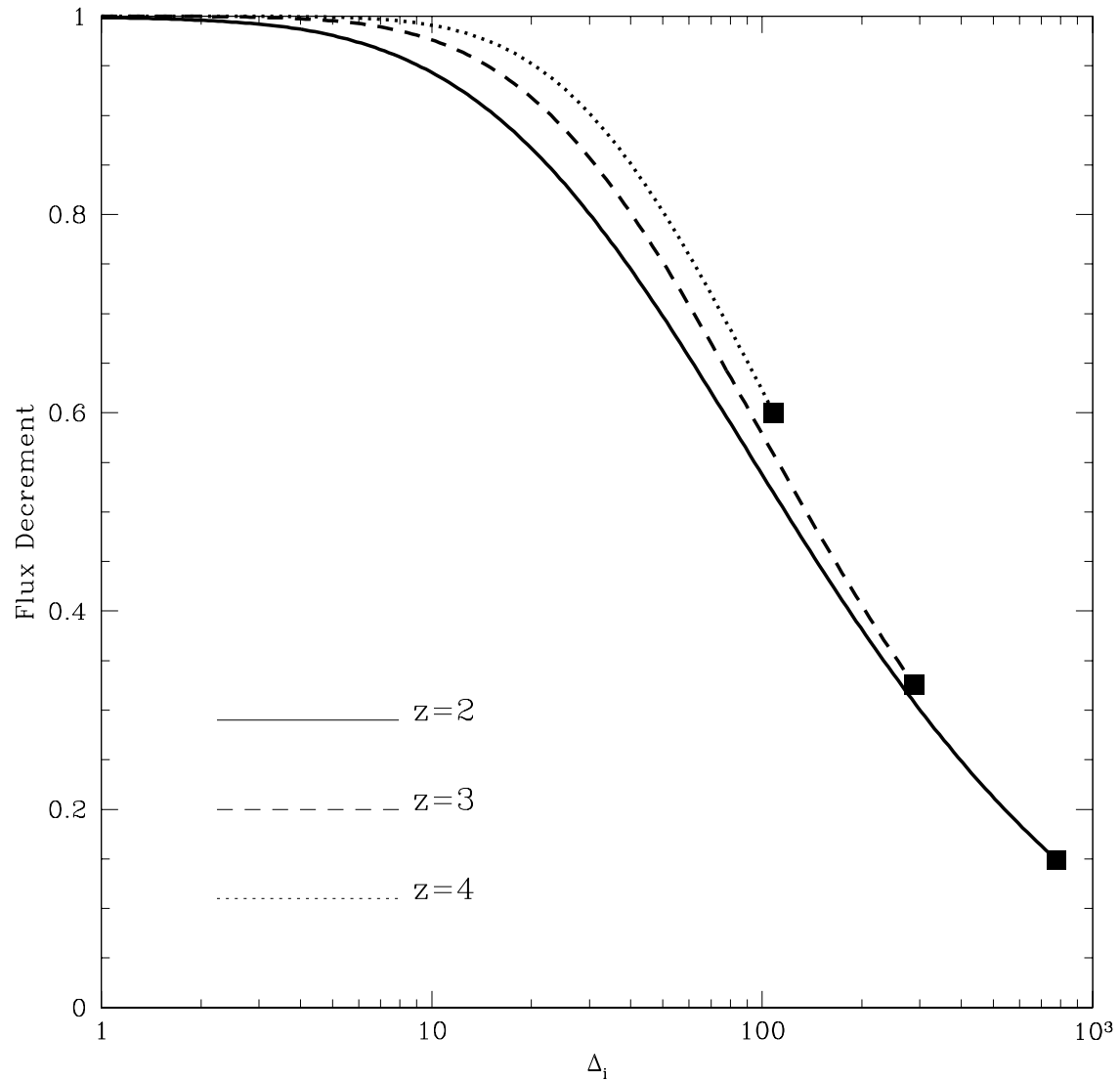


Fig. 5.— Mean flux decrement as a function of the overdensity up to which the gas is ionized. Solid squares indicate the observed value of the mean flux decrement according to Rauch et al. (1997) at $z = 2, 3, 4$.

of reionization is reached at this redshift, but because even the most underdense voids have a large enough density of neutral hydrogen to scatter essentially all the Ly α photons from a background source.

Nevertheless, the redshift at which the Gunn-Peterson trough is first seen might be higher if more sources were present at high redshift. For example, if the emissivity remained at $\epsilon \simeq 5$, then $\Delta_i \simeq 100$ at $z = 6$ and the flux decrement would not decline very fast at $z > 4$. In fact, because less mass has collapsed to high densities at high redshift, the value of Δ_i (and therefore the flux decrement) becomes extremely sensitive to R (Fig. 2d). However, our model of the density distribution does not take into account that dense gas could be present in low-mass halos that collapsed before the IGM was ionized, on scales below the Jeans scale of the photoionized gas.

The observations of the highest redshift sources (Dey et al. 1998, Weymann et al. 1998) suggest so far that the flux decrement rapidly declines, indicating that the decrease of Δ_i with redshift probably continues along the same trend shown in Figure 5 at higher redshifts.

3.4. The mean free path and the abundance of Lyman limit systems

Figure 6 shows the mean free path λ_i as a function of Δ_i that we derive in our model. For the values of Δ_i obtained previously to match the observed flux decrement, the mean free path at $z = (2, 3, 4)$ is $H \lambda_i = (50, 33, 18) \times 10^3 \text{ km s}^{-1}$, which is in good agreement with the number of observed Lyman limit systems per unit redshift, $\sim 2[(1+z)/4]^{1.5}$ (e.g., Storrie-Lombardi et al. 1996). We notice that in the MCOR simulation, the number of Lyman limit systems was much less than observed. The reason we obtain a good match here is because we have fitted the high-density tail of the density distribution with a power-law that is close to an isothermal slope for gas distributed in halos, and we have also used a power-law dependence of λ_i on Δ_i that assumes the presence of halos with density cusps. The numerical simulation in MCOR contains instead halos of gas with core sizes limited by the resolution, which explains why the number of Lyman limit systems in the simulations was smaller than in our model here.

3.5. Gaps in the Gunn-Peterson trough due to individual H II regions

Is it possible that some of the last gaps of transmitted flux appearing in Ly α spectra will correspond to individual H II regions around the sources that reionized the IGM before the epoch of overlap? As pointed out in Miralda-Escudé (1998, hereafter M98), there are

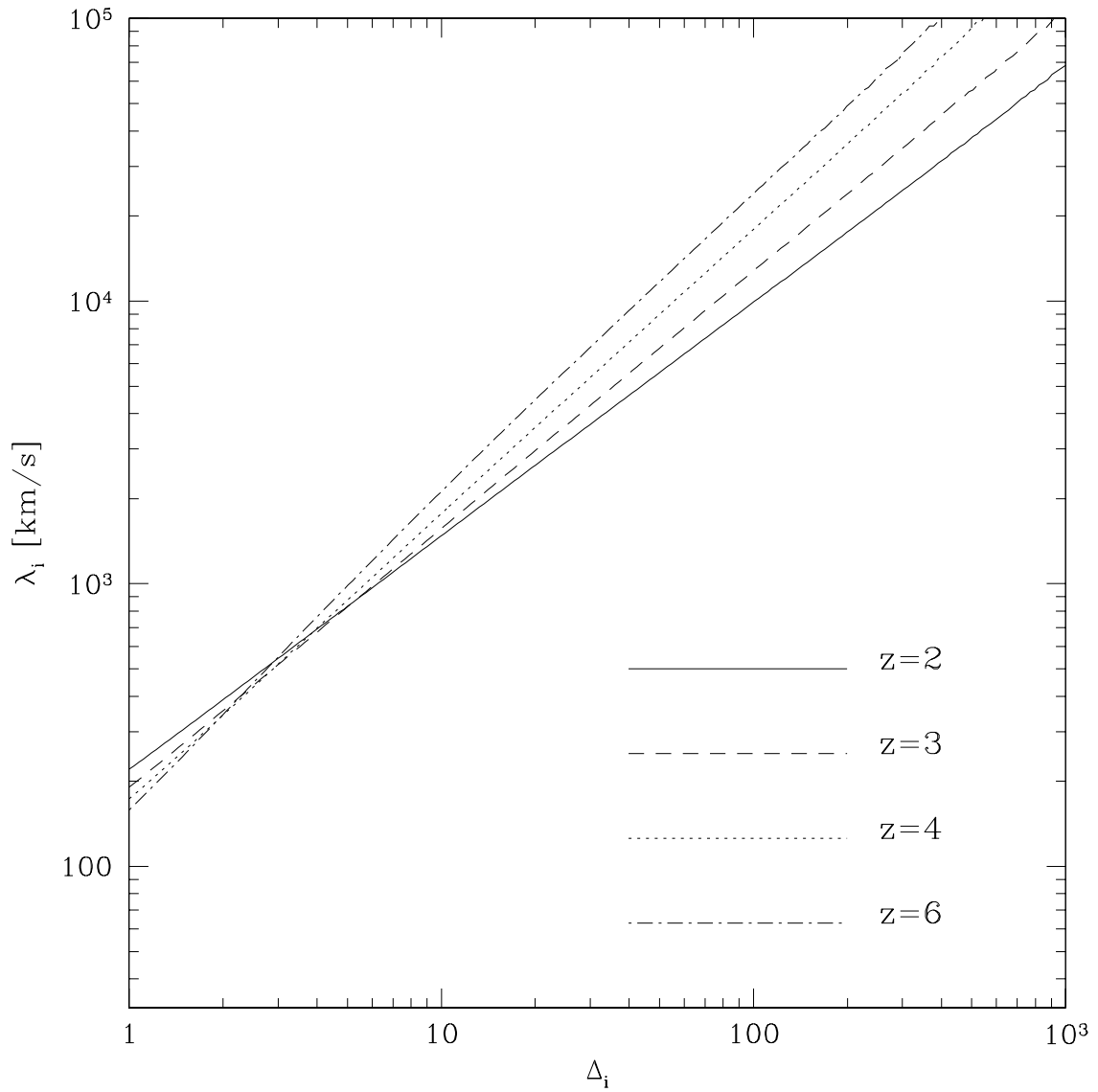


Fig. 6.— Mean free path of ionizing photons as a function of the overdensity up to which the gas is ionized, according to equation (8), at the indicated redshifts.

two conditions that need to be satisfied for an ionized region to transmit flux. The first condition is the one we have also discussed here: the optical depth through the ionized region should not be much higher than unity. Given the discussion at the end of §2, the formalism developed here to compute the typical value of τ_i from equation (11) should be equally valid before the epoch of overlap, in H II regions around individual sources, taking into account the following differences: (a) The mean emissivity is now substituted by ϵ/Q_i , averaging only over the ionized volume of the universe. (b) The mean free path λ_i should be identified with the radius of the H II region. (c) The fluctuations of the intensity should be much higher than after the epoch of overlap, so when the line of sight passes near a luminous source τ_i may be decreased owing to a high value of f_J in equation (11).

From Figure 4, we see that the transmitted flux rapidly becomes very small when the optical depth of a uniform IGM with the same intensity of the ionizing background is $\tau_u \gtrsim 50$. For our model of the mean free path, this corresponds to $\Delta_i \lesssim 20$, and $H(z)\lambda_i \lesssim 4000 \text{ km s}^{-1}$ near $z = 6$. This condition is equally applicable to individual H II regions: in order for an H II region to be visible in the Ly α spectrum as a gap in the Gunn-Peterson trough, the mean intensity of radiation in the H II region should be large enough to make $\tau_u \lesssim 50$, implying (for $z = 6$) that the gas must be ionized up to densities $\Delta_i \sim 20$ in order for the ionized region to be at least as big as the mean free path $\lambda_i \sim (4000 \text{ km s}^{-1})/H(z)$ given by Figure 6. The spectrum of the line of sight through an H II region of at least this size will then show a gap in the transmitted flux when voids are crossed with the average ionizing intensity given by the luminosity of the source and the size of the ionized region. Smaller H II regions can be seen only rarely if the line of sight passes through a void close to the source (so that $f_J \gg 1$).

The second condition for an isolated H II region to transmit any Ly α photons arises from the fact that if a large fraction of the IGM is still neutral, then the damped absorption profiles of the neutral gas in front and behind the H II region will overlap, scattering the remaining photons that could have crossed an underdense, ionized region. It was shown in M98 that an H II region must have a proper size larger than $1h^{-1}[\Omega_b h(1 - Y)/0.03] \text{ Mpc}$ to prevent this overlap of damping wings, and that the optical depth in an H II region of this size is $\tau_u = 475(T/10^4 \text{ K})^{-0.7} \epsilon^{-1}$ (see eq. 4 in M98; the quantity N_r in M98 is $2n_b/3n_e$ times our ϵ , where $n_e/n_b = 1 - Y/2$), independently of the redshift or any other parameters. In general, this condition is not as restrictive as the first one, $\tau_u \lesssim 50$, needed for the ionized region itself to have a low enough optical depth, if we assume $\epsilon \simeq R \simeq 2$ at $z = 6$. However, for small H II regions this second condition implies that even if the gap of transmitted flux could be visible due to $f_J \gg 1$, the flux might still be removed due to the damping wings.

We therefore conclude that whether Ly α photons can be transmitted before the overlap

of H II regions is complete depends mainly on the typical luminosity of the sources of ionizing photons. We shall discuss plausible sizes of the H II regions in §4.

This section has presented a general formalism to calculate the evolution of τ_u with redshift, the epoch when the Ly α forest should become a complete Gunn-Peterson trough, and the condition on the size of the individual H II regions required for Ly α flux to be transmitted through them. However, our numerical results depend on the density distribution $P_V(\Delta)$ and the scale of the density structures in the IGM, λ_0 , which we have taken as constant in redshift space here. These quantities will need to be calculated separately for every cosmological model as a function of redshift.

4. Hydrogen Reionization

4.1. Sources of Ionizing Radiation : QSO's and Galaxies

Among known, observed objects, QSO's and galaxies are the two candidates for the sources of ionizing photons that reionized the IGM. At $z \simeq 3$ the total number of UV photons emitted by galaxies longward of the Lyman break outnumbers those produced by optically bright QSO's by a factor of approximately ten to thirty (Boyle & Terlevich 1998; Haehnelt, Natarajan, & Rees 1998). For photons capable of ionizing hydrogen, the balance is less certain. Observed bright, high-redshift QSO's show no Lyman break, whereas galaxies have a strong intrinsic Lyman break arising from the stellar atmospheres (of a factor ~ 5 for the usual mass function of stars observed in galaxies), and a very uncertain escape fraction of photons beyond the Lyman edge. For starbursts at low redshift, the escape fraction is reported to be of order 10% (Leitherer et al. 1995; Hurwitz, Jelinski & Van Dyke Dixon 1997). A moderately higher value would therefore be required for UV emission by star-forming galaxies to rival that of QSO's at $z = 3$ in terms of ionizing photons.

The solid curves in Figure 7 show a fit to the luminosity function of QSO's at $z = 4$ obtained by Pei (1995): $d\Phi = \Phi_*/((L/L_*)^{\beta_1} + (L/L_*)^{\beta_h}) dL/L_*$, with $\Phi_* = 8.9 \times 10^{-7} \text{ Mpc}^{-3}$, $L_* = 7.8 \times 10^{45} \text{ erg s}^{-1}$ (B-band) and $\beta_h = 3.52$. The luminosity function is plotted as follows: on the horizontal axis, instead of the luminosity L , we use the variable $R_{\text{HII}} = [3N_{\text{phot}}/(4\pi n_{\text{H}})]^{1/3}$, where N_{phot} is the total number of ionizing photons emitted by the source for an assumed lifetime t_Q , n_{H} is the comoving number density of hydrogen, and R_{HII} is the comoving radius of the H II region that a source of luminosity L would produce in a completely neutral homogeneous medium if there were no recombinations. We obtain the number of photons from the relation $N_{\text{phot}} = Lt_Q/E_{\text{ion}}$, where E_{ion} is the mean energy per photon. We have assumed that the QSO's emit twice the luminosity in ionizing photons

as in the B-band (a reasonable approximation for the typical observed quasar spectra), and have used $E_{\text{ion}} = 20 \text{ eV}$. Also shown in the upper horizontal axis is the corresponding expansion velocity at $z = 4$, $H(z = 4) R_{\text{HII}} / (1 + 4)$.

On the vertical axis, the mean comoving volume emissivity of QSOs per unit natural logarithm of R_{HII} is plotted, in terms of the number of photons emitted per hydrogen atom per Hubble time. The curves in Figure 7 are an “energy function” (or the distribution of total energy emitted by sources), rather than a luminosity function. The energy function depends of course on the assumed lifetime, and we have plotted it for two values: $t_Q = 3 \times 10^7 \text{ years}$ and $t_Q = 8 \times 10^8 \text{ years}$. For other values of t_Q , the curves simply shift horizontally by a factor proportional to $t_Q^{1/3}$. The time $8 \times 10^8 \text{ years}$ is equal to half the age of the universe at $z = 4$; this can be considered as an upper limit for t_Q , because the number of quasars of given luminosity should be rapidly increasing with time at high redshift. All values are computed for our adopted cosmological model mentioned in the introduction.

The faint end slope of the luminosity function is still rather uncertain, so we have plotted three curves for the values $\beta_l = (1.5, 1.65, 1.8)$, where $\beta_l = 1.64$ is the value preferred by Pei. The value of the lowest luminosity for which the abundance of quasars has been determined observationally at $z = 4$, $10^{46} \text{ erg s}^{-1}$, is indicated with an arrow. For lower luminosities, the model assumes that the luminosity function has the same shape as at lower redshift.

The diamond symbols in Figure 7 show in the same way the mean comoving volume emissivity of UV-emitting galaxies. We use a Schechter function fit to the luminosity function at $z = 3$ (Dickinson et al. 1998), $d\Phi = \Phi_* (L/L_*)^\beta \exp(-L/L_*) dL/L_*$, with $\Phi_* = 1.6 \times 10^{-3} \text{ Mpc}^{-3}$, $L_* = 1.4 \times 10^{44} \text{ erg s}^{-1}$ (defined as $\nu L_{*\nu}$ at 1500 Å), and $\beta = -1.5$. The luminosity function of UV-emitting galaxies does not evolve strongly between $z = 3$ and $z = 4$ (Steidel et al. 1998). The ionizing luminosity is assumed to be a fraction 0.06 of νL_ν at 1500 Å, due to an intrinsic Lyman break of a factor 5, and assuming a fraction of 30 % of emitted ionizing photons to escape into the IGM. The age of the galaxies is set equal to $8 \times 10^8 \text{ years}$, or half the age of the universe at $z = 4$.

The integrals under the curves of the energy functions give us the total emissivity, in terms of number of emitted photons per hydrogen atom per Hubble time. For both QSO’s and galaxies, their total emissivity at $z = 4$ is $\epsilon \sim 5$. The radii of the H II regions when the lifetime is set to $t_S \equiv (\epsilon H)^{-1}$ have a special significance: over the time $(\epsilon H)^{-1}$, one ionizing photon is emitted for each atom in the universe, and therefore the H II regions around each source are just large enough for overlapping. Therefore, for this lifetime, the variable in the horizontal axis is equal to the radius that the ionized regions around a source of a given luminosity must have grown to at the epoch of overlap, when reionization ends. The curve

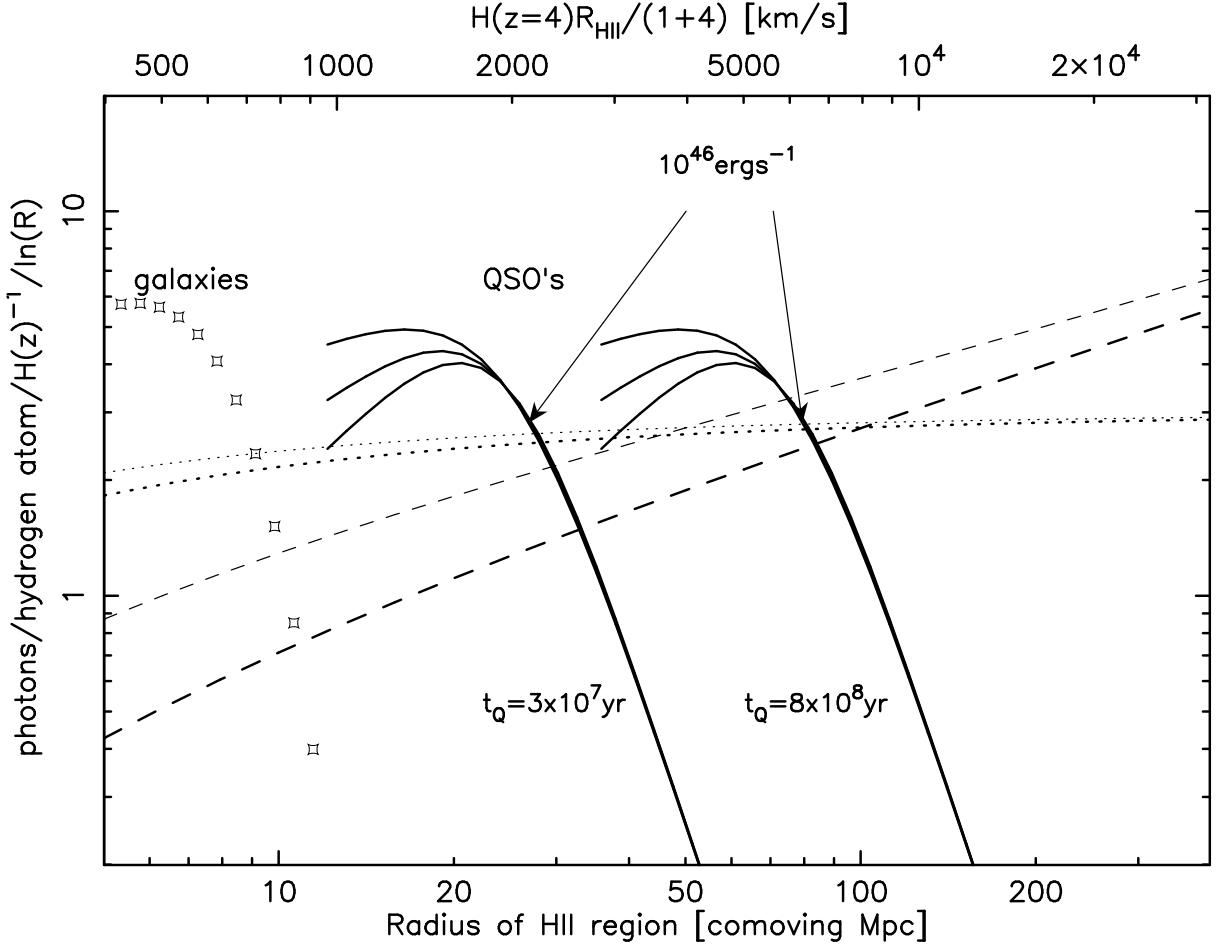


Fig. 7.— The solid curves show the mean comoving volume emissivity from QSOs in terms of the number of ionizing photons emitted per hydrogen atom per Hubble time as a function of the comoving radius of the reionized region created by a quasar over a lifetime t_Q , if recombinations are ignored. The QSO luminosity function at $z = 4$ of Pei (1995) is used. The three curves in each set are for faint end slopes $\beta_1 = (1.5, 1.65, 1.8)$. The open diamond symbols show the mean comoving volume emissivity of star-forming galaxies at $z = 4$ calculated from the luminosity function according to Dickinson et al. (1998). An intrinsic Lyman break of a factor five and an escape fraction of ionizing photons of 30 percent is used to extrapolate from the flux at 1500 Å and a lifetime $t_Q = 8 \times 10^8$ yr is used. The arrows denote the radii which correspond to a $10^{46} \text{ erg s}^{-1}$ QSO. The dashed lines show the global number of recombinations taking place per Hubble time and per hydrogen atom as a function of the mean free path (equated to the HII region radius in the bottom axis) at redshifts $z = 4$ and $z = 6$. The recombination rate was calculated as described in §3 for the density distribution shown in Fig. 1. The dotted curves give the mass fraction required to ionize up to the overdensity corresponding to that mean free path, times a factor 3.

corresponding to this lifetime would be shifted to the left from the curve for $t_Q = 8 \times 10^8$ yr by a factor $(5/3)^{1/3} = 1.19$.

The requirement for having completed the reionization with a given population of sources can now be easily visualized from Figure 7. We shall consider first the case of long-lived sources that remain active with an approximately constant luminosity over the epoch of reionization; the differences in the case of short-lived sources will be discussed later. In the previous sections we computed the global recombination rate in terms of the maximum overdensity to which the universe is reionized, Δ_i , which in turn can be expressed in terms of the mean free path λ_i (using equations [1], [6], and [8]). The dashed lines in Figure 7 give the number of recombinations taking place per Hubble time as a function of λ_i , equated here to the radius of the H II region in the bottom axis. The dotted curves give the mass fraction F_M required to ionize the IGM up to the overdensity corresponding to the mean free path λ_i , times a factor 3. These curves are shown at $z = 4$ (thick lines) and $z = 6$ (thin lines). At high redshift, the emissivity from quasars could of course be different, depending on how they evolve. At the epoch of overlap, the radii of the H II regions must have grown to the values given in Figure 7 for the lifetime $t_S = (\epsilon H)^{-1}$. The first condition necessary to reach the epoch of overlap is that $\epsilon t_R H > F_M$, where t_R is the time during which sources have been producing the emissivity ϵ , and $\epsilon t_R H$ is the total number of photons emitted. Choosing $t_R = (3H)^{-1}$ (i.e., half the age of the universe at the epoch of overlap), this condition becomes $\epsilon > 3F_M$, roughly equivalent to requiring that the solid line for a lifetime t_S should be above the dotted line in Figure 7. The second condition is that the global recombination rate when the mean free path is equal to the size of the H II regions that must be reached for overlap is not greater than the emissivity. This condition roughly implies that the solid line must be above the dashed line.

As the emissivity of the sources increases, the epoch of overlap is reached when the mean emissivity of the sources rises above both the dashed and dotted lines. This shows that *the importance of recombinations, and the required emissivity to reionize the IGM, increases not only with redshift but also with the luminosity of the sources.*

For sources with luminosities typical of high-redshift starburst galaxies, the fact that the dashed line is below the dotted line implies that recombinations should not be very important in the case of late reionization by galaxies. Even if very luminous QSO's reionized the universe, recombinations increase the required number of emitted photons by a moderate factor only, because the IGM does not need to be ionized up to a very high overdensity to increase the mean free path up to the size of the H II regions produced by these sources. Recombinations are of course more important as the redshift of reionization is increased.

Now, we consider the case of short-lived sources, with lifetimes much less than t_R . As the reionization proceeds, the IGM should contain active H II regions, which continue to expand as more radiation is emitted by the source, and fossil H II regions, which start recombining after their central source turns off, but are still mostly ionized. This implies that in the case of short-lived sources there are two different epochs of overlap, a first one for the overlap of fossil H II regions, and a second one for the overlap of active H II regions. The first epoch of overlap of fossil H II regions is determined by the energy function of sources. This occurs when the emissivity rises above the dashed and dotted lines at the value of the mean free path equal to the radius of fossil H II regions, determined by the lifetime t_Q . The second epoch of overlap is determined by the luminosity function, and it generally occurs significantly later and requires a higher emissivity, determined by the same condition as for long-lived sources obtained when the solid lines are shifted to the right to the lifetime $t_S = (\epsilon H)^{-1}$. Between these two epochs of overlap, the emitted ionizing photons are invested not just in ionizing again the baryons that have recombined in fossil H II regions, but in ionizing additional gas in more overdense regions in order to increase the mean free path to the separation between active H II regions. The shorter the lifetime of the sources, the more widely separated the two epochs of overlap become.

In the example of a lifetime $t_Q = 3 \times 10^7$ years, fossil H II regions overlap when a typical quasar with luminosity $10^{46} \text{ erg s}^{-1}$ has produced an H II region of comoving radius 25 Mpc. The overlap of active H II regions would be reached only when the radius of H II regions around a quasar of this luminosity increases up to a radius of 70 Mpc, requiring a higher emissivity to balance the global recombination rate.

It is clear from Figure 7 that for both QSO's and galaxies, the emissivity is sufficient to have reionized the universe by $z = 4$. If we use the approximation $\epsilon = R$, our model predicts that at $z = 4$, $\Delta_i = 100$ and $R \simeq 6R_u \simeq 4$ (see Figs. 2c, 5), so the combined emissivity of quasars and galaxies can actually be slightly higher than what is needed to match the observed flux decrement. At higher redshifts, the dashed line indicating the recombination rate increases and also becomes shallower, and the epoch of reionization is reached when the dashed line is equal to the emissivity at the mean separation between the sources. If the emissivity from low-luminosity galaxies remains at a constant level, this may not happen until $z \simeq 10$ or higher. To make further progress, a determination of the escape fraction of ionizing photons from high-redshift galaxies and of the number densities of faint quasars and galaxies at high redshift will be required.

4.2. The Size of H_{II} Regions at the Epoch of Reionization

We now come back to the question of the possible presence of gaps of transmitted flux due to individual H_{II} regions in Ly α spectra of high-redshift sources before the hydrogen reionization is completed. In §3 we showed that these gaps should generally be present if $\tau_u \lesssim 50$, which for our value of the mean free path corresponds to a size of the H_{II} region of $H \lambda_i \gtrsim 4000 \text{ km s}^{-1}$, or $(1+z)\lambda_i \gtrsim 40 \text{ Mpc}$ at $z \simeq 6$; smaller H_{II} regions can also produce gaps when $f_J > 1$. At higher redshifts, the required size of the H_{II} regions to produce a gap of transmitted flux increases, both due to the lower underdensities of voids, and to the longer mean free path at fixed τ_u (see Figures 3, 5 and 6).

Figure 7 shows that the typical QSO’s that dominate the emissivity at $z = 4$ are able to create H_{II} regions large enough to produce observable gaps in Ly α spectra. In the case of short-lived QSO’s, the H_{II} regions would be smaller at the first epoch of overlap of fossil regions. However, when the active H_{II} regions overlap, their size obviously depends only on the observed luminosity function of active sources, and not on their lifetimes. Star forming galaxies do not reach the required size, and therefore their associated H_{II} regions can only be visible in cases where f_J is large. We notice here that the conclusion in M98 that these gaps of transmitted flux would probably not be present at redshifts above the epoch of overlap was due to assuming that the high-redshift sources responsible for reionization would be of low-luminosity compared to the known QSO’s at lower redshift.

The size of H_{II} regions at overlap has strong implications for the effect of reionization on the fluctuations of the CMB background (e.g. Gruzinov & Hu 1998). Unfortunately the constraints are extremely weak. The typical size could range from less than 1 Mpc if faint star-forming galaxies were the ionizing sources to several tens of Mpc if reionization were caused by bright QSO’s.

5. Helium Reionization

The double reionization of helium can be treated following the same method we have used for hydrogen. The He_{III} recombination rate is 5.5 times faster than that of hydrogen (this is increased to 5.9 times faster when including the increase in the electron density due to the ionization of helium), $R_{\text{HeIII},u}(z) = 0.21 [\Omega_b h(1 - Y/2)/0.027] (1+z)^{3/2}/\Omega_0^{1/2}$. If the number of photons emitted above the He_{II} ionization threshold is not higher than $5.9n_{\text{He}}/n_{\text{H}} = 0.46$ times the number of photons emitted above the hydrogen ionization edge (which is the case for all existing candidates of the sources of the ionizing background), and if recombinations are the dominant balance to the emissivity, then the He_{II} should be

reionized at a later epoch than the hydrogen.

Equations (1), (3), (4), and (8) are equally applicable for He II, once we define the new quantities ϵ_{He} and $n_{J,\text{He}}$ as the emissivity per Hubble time and the number density of photons above the He II ionization edge for each helium atom, and Δ_{He} as the density below which helium starts being doubly ionized. Equation (12) is also equally valid, except that the numerical factor changes from 1.14 to 1.23 (due to the ratio of the number of hydrogen atoms to the total number of hydrogen and helium atoms that is included in this equation for the case of hydrogen); the basic reason is that the ratio of the integrated optical depths to Ly α line scattering and to continuum ionizing radiation is always the same for a H II or a He III region.

Figure 8 shows τ_u versus Δ_{He} , and Figure 9 shows the flux decrement, at redshifts $z = 2, 3, 4$ (the latter is obtained directly from the numerical simulation in MCOR [see their Fig. 19], and it includes the effect of thermal broadening of helium). The symbols in Figure 9 show the observed mean flux decrement in the following objects: triangle, Q0302 – 003 at $z = 3.15$ (Heap et al. 1999); square, Q0302 – 003 at $z = 2.82$ (Heap et al. 1999); hexagon, HS1700+64 at $z = 2.4$ (Davidson et al. 1996). The value of Δ_{He} indicated by each point in Figure 9 gives the overdensity of the gas up to which helium should be doubly ionized, in order to reproduce the flux decrement in our model. The implied mean free path of the He II -ionizing photons can then be read off Figure 6.

The results of the observations of the He II Ly α spectra can be summarized as follows: a flux decrement has been clearly detected in four quasars, which increases rapidly with redshift over the range $2.2 < z < 3.2$. At the upper end of this range, a very small fraction of the flux is transmitted over most of the spectrum, but there are gaps (with widths $\sim 1000 \text{ km s}^{-1}$) where the fraction of transmitted flux is high (Reimers et al. 1997, Anderson et al. 1998; Heap et al. 1999). Some of the wide gaps can be associated with the proximity effect of the observed sources; however, other gaps are far from the sources. According to Heap et al. (1999), outside of these gaps a very small fraction of transmitted flux of $\sim 1\%$ is detected up to the highest redshift observed (corresponding to the triangle in Fig. 9).

Figure 10 is analogous to Figure 7, showing the emissivity of He II -ionizing photons per helium atom from quasars as a function of the comoving radii of their He III regions, at $z = 3$, plotted for two assumed lifetimes: 3×10^7 and 10^9 years (the latter is \sim half the age of the universe at $z = 3$). The top horizontal axis gives the Hubble velocity corresponding to the radius of the He III region at $z = 3$. We use again the parameterization of the QSO luminosity function given by Pei (1995). As before the dashed line shows the global recombination rate per helium atom. We have assumed a spectral index of $\gamma = 1.8$ ($f_\nu \propto \nu^{-\gamma}$) to extrapolate from the hydrogen to the helium Lyman continuum (Zheng et al.

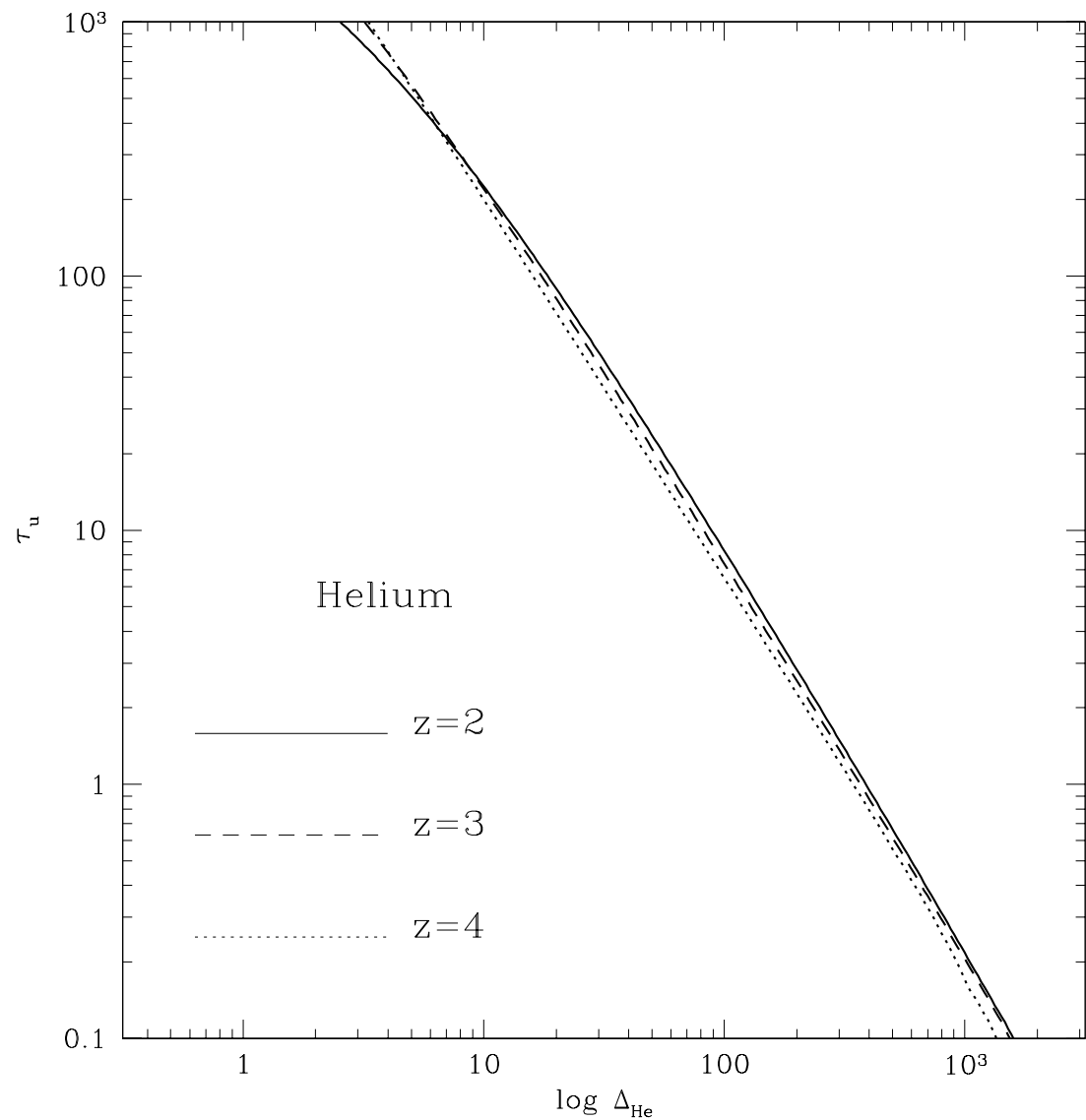


Fig. 8.— Same as Fig. 3, for the case of helium.

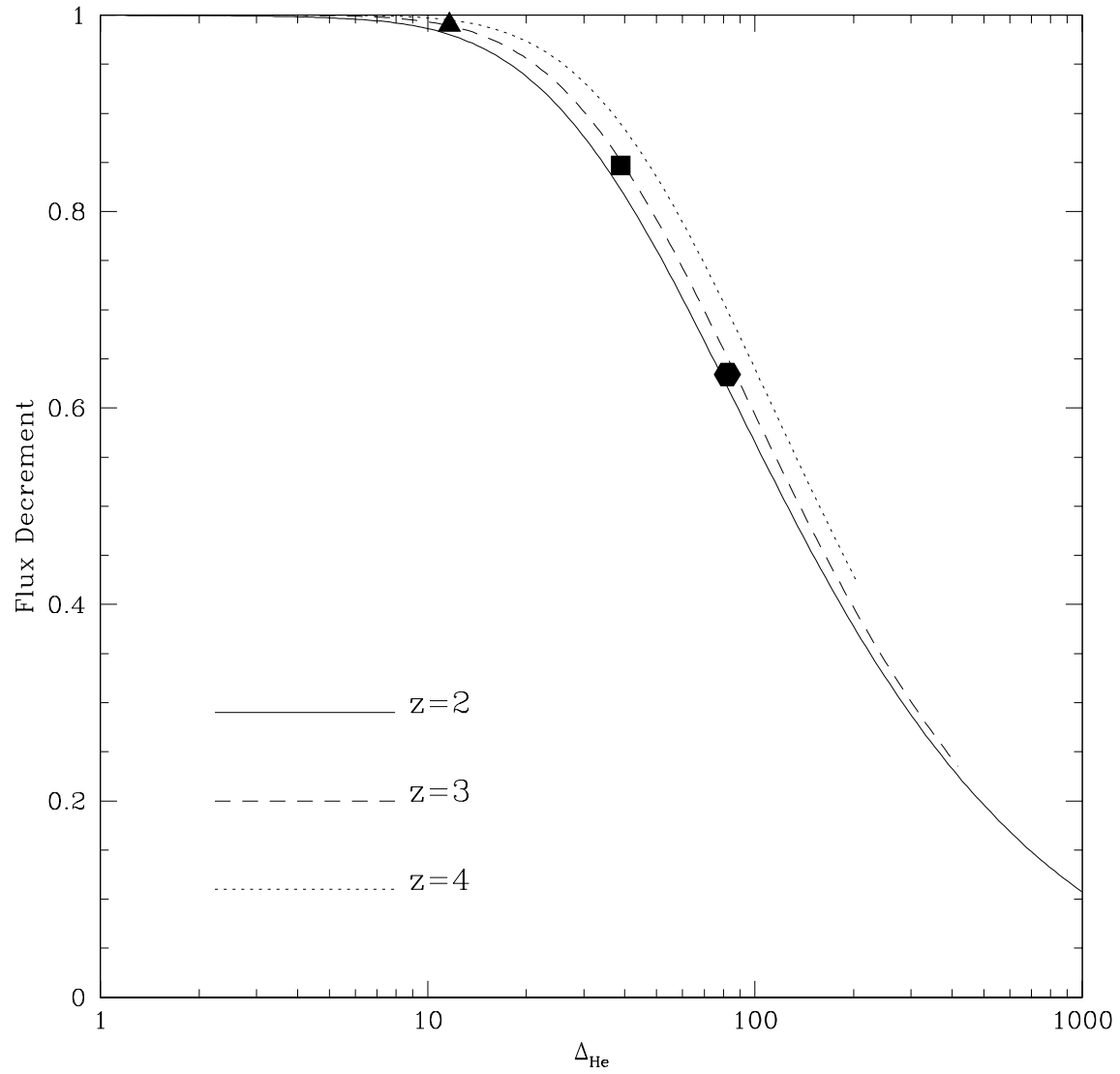


Fig. 9.— Mean flux decrement as a function of the overdensity up to which the gas is ionized, for the case of helium. Symbols indicate the observed mean flux decrements in the objects specified in the text.

1997).

According to our model, the total emissivity of QSO's is sufficient to completely reionize He II before $z = 3$, since the emissivity is above the global recombination rate for the lifetime $t_S = (\epsilon_{He} H)^{-1} \simeq 1.7 \times 10^8$ yr. The mean free path should be given by the radius where the emissivity equals the recombination rate, $\lambda_{He} \sim 7000 \text{ km s}^{-1}$, corresponding to $\Delta_{He} \sim 50$ according to Figure 6. This then implies a flux decrement ~ 0.8 from Figure 9; in addition, since the mean free path should already be larger than the separation between the quasars dominating the emissivity, fluctuations in the intensity of the background should be relatively small. These predictions seem to fit the observational results at a slightly lower redshift, $z \simeq 2.5$. On the other hand, the observations of a much larger flux decrement with gaps of transmitted flux at $z \simeq 3$ suggest a lower emissivity than in the model by Pei used in Figure 10.

A model for the sources of He II -ionizing radiation that reproduces the observations at $z \simeq 3$ should have a population of low-luminosity sources that has ionized the He II up to overdensities $\Delta_{He} \simeq 12$, to reproduce the transmitted flux reported by Heap et al. (1999) outside the large gaps. From Figures 6 and 10, this implies a mean free path $\lambda_{He} \simeq 1500 \text{ km s}^{-1}$ and an emissivity $\epsilon_{He} \simeq 4$ from these low-luminosity sources. Luminous quasars should also have a similar emissivity ϵ_{He} , placing it slightly below the dashed line in Figure 10, allowing for the presence of numerous gaps of transmitted flux caused by regions that are more intensely ionized by luminous quasars. The presence of sources with a wide range of luminosities can allow for large fluctuations in the intensity of the background due to the most luminous sources, well after reionization has been completed by less luminous sources.

We notice here that, in the case of helium, recombinations are much more important than the need to ionize He II for the first time, for luminous sources (i.e., the dashed line is well above the dotted line in Fig. 10). Because the recombination rate grows rather steeply with the mean free path, low-luminosity sources are very likely to have ionized the He II entirely at $z > 3$. If the emissivity from sources with the abundance of galaxies in Figure 7 is more than 10% of the emissivity from luminous quasars, then galaxies should have reionized the He II first, since the recombination rates at the mean separation between galaxies and luminous quasars differ by a factor ~ 10 . It is quite plausible that the emissivity from galaxies reaches at least this level, because the cooling radiation from supernova remnants and hot gas in the halo produces photons of the right energy for the ionization of helium. Therefore, unless luminous quasars have always dominated by a large factor the emissivity of He II -ionizing photons, the He II should have been ionized by lower luminosity sources and the epoch of overlap of the He III regions should be earlier than

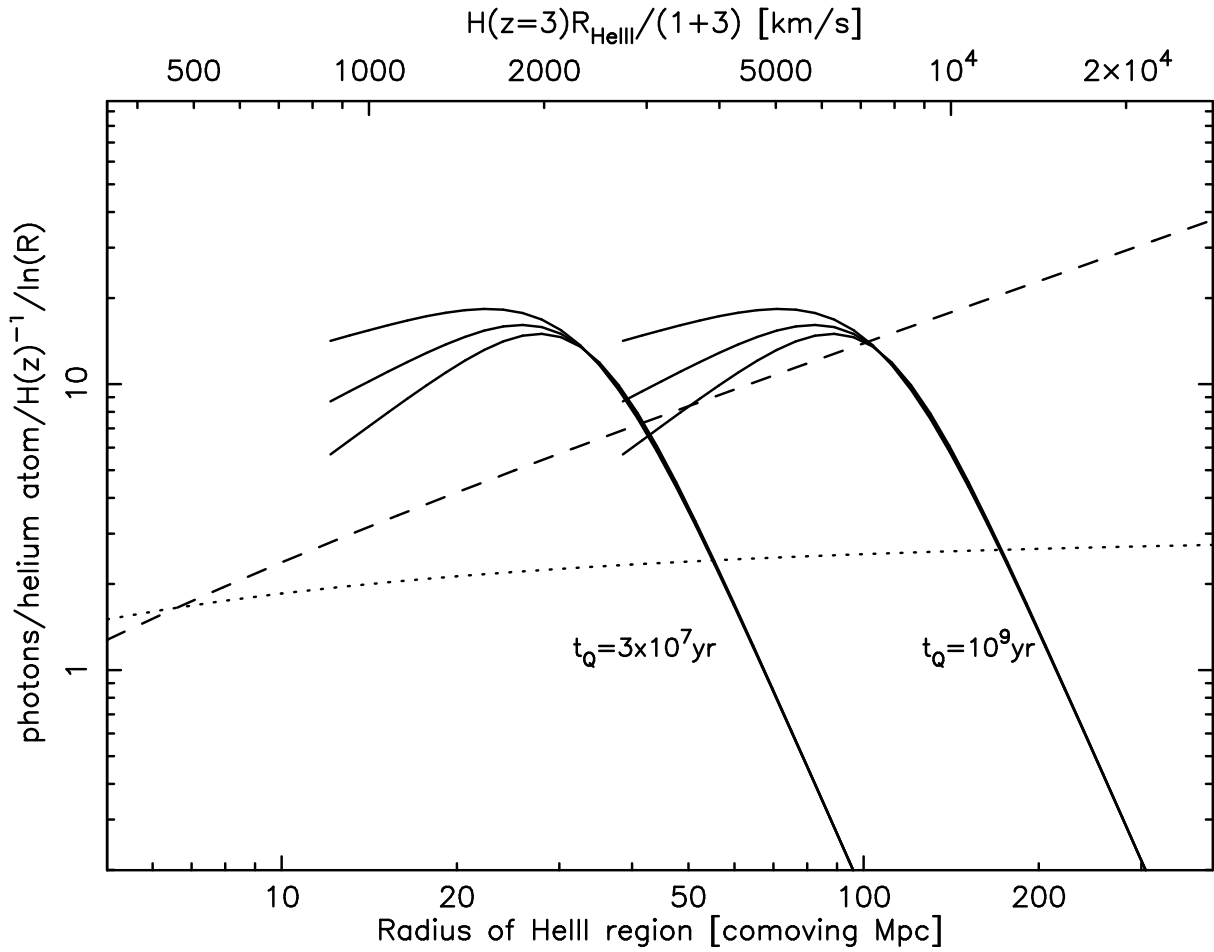


Fig. 10.— Same as Figure 7, for the case of helium, at $z = 3$. The emissivity from quasars is shown here in terms of number of photons emitted per Hubble time and per helium atom, as a function of the radius of the He III region that a quasar of lifetime t_Q would create in the absence of any recombinations.

$z = 3$.

Thus, our interpretation of the gaps of transmitted flux in the He II Ly α spectra is that they are due to an ionization effect of a luminous source, rather than simply a low density region in the IGM (which is supported by various tests presented by Heap et al. 1999), but that they are not truly He III regions before the epoch of overlap. Instead, the luminous quasars are only increasing the background intensity in a large region around them, and ionizing the dense gas in the absorption systems to greater depth. To illustrate this point, we can calculate the degree of ionization of the He II when $\Delta_{\text{He}} = 12$, and therefore the transmitted flux in the He II Ly α spectrum is only 1% according to Figure 9. As mentioned above, this requires an emissivity $\epsilon_{\text{He}} = 4$, a mean free path $H\lambda_{\text{He}} \simeq 1500 \text{ km s}^{-1}$, and an intensity $n_{\text{J,He}} = \epsilon_{\text{He}}(H\lambda_{\text{He}}/c) = 0.02$. The implied fraction of He II is $x_{\text{He II}} = \alpha_{\text{rmHe}} n_e / (\bar{\sigma}_{\text{He}} c n_{\text{He}} n_{\text{J,He}}) \simeq 10^{-1} \Delta$. Therefore, over most of the volume in the IGM where $\Delta < 1$, the He II fraction is already reduced to less than 10% by the low-luminosity sources. Within a gap where the transmitted flux is increased to 20%, we need $\Delta_{\text{He}} \simeq 50$ (Fig. 9), increasing the recombination rate by a factor 3 and the mean free path by a factor 4 (Figs. 6 and 10), and therefore the intensity by a factor 12, so the He II fraction is reduced to $x_{\text{He II}} \simeq 0.008 \Delta$.

Why might the emissivity from quasars be less than is estimated from the observations? One possibility is that the He II -ionizing radiation from many quasars is absorbed locally in their host halos, or near the nucleus. Only two of the four quasars for which the He II Ly α forest has been observed show the strong proximity effect that is expected (Anderson et al. 1998 and references therein). Among the quasars of lower luminosity that dominate the emissivity, a greater fraction of the radiation could be locally absorbed. Another possibility is that the value of Ω_b is higher than predicted by nucleosynthesis for the deuterium abundance found by Burles & Tytler (1998).

Songaila & Cowie (1996) have reported a decrease of the Si IV/C IV ratio with increasing redshift for intermediate column density hydrogen Ly α absorption lines (see also Boksenberg 1998). Songaila & Cowie interpreted this evolution as a softening of the spectrum with increasing redshift and argued for a rather sudden reionization of He III at $z \simeq 3$. As discussed in §3, reionization is expected to be gradual, and we should therefore expect a progressive decrease of the intensity of the He II -ionizing background with redshift, as the He II photon mean free path decreases. Heap et al. (1999) mentioned that a sudden change of the intensity of the He II -ionizing background at $z \simeq 3$ is supported by the sudden change in the mean transmitted flux in the He II Ly α spectra. This sudden change in the mean transmitted flux may be due to two reasons: first, as seen in Figure 9, even if Δ_{He} decreases smoothly with redshift, the flux decrement reaches unity very rapidly because the

voids have a minimum value of their densities $\Delta \simeq 0.1$, as we discussed earlier for the case of hydrogen. Second, simple Poisson fluctuations in the number of gaps caused by luminous sources may explain the apparently sudden change in the filling factor of these gaps near $z = 3$, since the He II Ly α spectrum has been observed in only four quasars.

A gradual reionization is also favored by the more recent results of Boksenberg, Sargent, & Rauch (1998), where a smooth evolution of the ratios Si IV/C IV and C II/C IV is reported, and also by the findings of Davé et al. (1998) who used the observed O VI absorption to argue that at least 50 percent of the volume of the universe at redshift near three is illuminated by a hard spectrum with significant flux well above the He II Lyman edge.

The reionization of He II can affect the evolution and spatial distribution of the temperature in the IGM (Miralda-Escudé & Rees 1994). Each helium atom yields an energy input of $\sim 54/(\gamma - 1)$ eV. For $\gamma = 1.8$, this results in a temperature increase of 20000 K during reionization, which affects the subsequent thermal history of the gas while the cooling is long compared to the Hubble time. The equilibrium temperature of photoionized gas may also fluctuate substantially owing to the heating by helium photoionization, on the scales of the regions of increased He II ionization around luminous quasars at $z \sim 3$. These temperature fluctuations could affect the evolution of the IGM and the formation of low-mass galaxies, because the collapse of the gas is significantly slowed down in halos of low velocity dispersion (see e.g., Efstathiou 1992, Thoul & Weinberg 1996). In the likely case where the ionizing radiation from a quasar is anisotropic, the present distribution of dwarf galaxies might show a large quadrupole moment around the locations of ancient quasars, probably occupied today by massive clusters of galaxies. These special galaxy fluctuations, which would constitute a new type of non-local galaxy bias unrelated to the primordial fluctuations, might be detected in future galaxy redshift surveys on the very large scales that He III regions can reach, where the amplitude of primordial fluctuations is greatly decreased.

6. Discussion and Conclusions

We have discussed in this paper how the clumpiness of the matter distribution and the discreteness of ionizing sources affects the reionization of hydrogen and helium and the appearance of the absorption spectra of high-redshift sources. In a clumpy medium, the underdense regions filling most of the volume of the universe will be reionized first, while the denser regions are gradually ionized later from the outside. As the emissivity increases, a balance is maintained with the global recombination rate by increasing the mean free

path of ionizing photons, as the size of the neutral, self-shielded regions at high density (which are observed as Lyman limit systems) shrinks.

The first gaps in the hydrogen and helium Gunn-Peterson trough in the absorption spectra of high-redshift objects should be caused by the most underdense voids. As the redshift is increased, the transmitted flux in Ly α spectra decreases rapidly not only because the intensity of the ionizing background diminishes if the emissivity from sources is lower, but also because the global recombination rate increases, and the voids are less underdense as predicted by the gravitational evolution of large-scale structure. We showed that if the emissivity does not increase with redshift at $z > 4$, then the Gunn-Peterson trough should be reached at $z \simeq 6$. This redshift is determined by the fact that the most underdense voids become optically thick to Ly α photons. However, the low-density IGM is likely to have been ionized everywhere at this redshift already, and the epoch of overlap of the H II regions around individual sources could have occurred at a substantially higher redshift if the emissivity is dominated by sources of low luminosity. The rapid increase of the He II Ly α flux decrement at $z \simeq 3$ can be similarly explained.

Whether it will be possible to see gaps of transmitted flux in a Ly α spectrum across the Gunn-Peterson trough, produced by individual H II regions around ionizing sources before the major fraction of the volume of the universe is reionized, depends on the luminosity of the sources. For a QSO with luminosity 10^{46}erg s^{-1} at $z = 6$, creating an H II region of radius ~ 70 comoving Mpc, the mean transmitted flux through the H II region would only be 10% (from Figures 5 and 6), and this transmitted flux decreases rapidly for sources of lower luminosity. If luminous quasars exist but are short-lived, there should be a first epoch of overlap of fossil H II regions (where the size of the H II regions would be smaller by a factor $(t_Q \epsilon H)^{1/3}$ relative to the case of long-lived sources), and a second epoch of overlap of active regions, having a size depending only on the luminosity of the quasars.

Smaller H II regions can on rare occasions produce gaps of transmitted flux when the intensity of radiation is much higher than average, when an underdense void that is close to the source compared to the size of the H II region is intersected by the line of sight. This should of course happen in the case of the “proximity effect”. For an H II region with proper radius smaller than 1 Mpc surrounded by neutral IGM, any residual flux that might be transmitted in these circumstances would still be absorbed in the damping wings of the absorption by the neutral IGM (see M98).

Reionization might be complete at a substantially earlier time than the redshift were the Gunn-Peterson trough is first encountered, if it is produced by low-luminosity sources. We have argued that this is likely to be the case for the He II reionization, where only a modest emissivity from low-luminosity sources is required to reionize the He II in small

He III regions well before the much larger He III regions produced by luminous QSO's can overlap. The presence of this low-luminosity sources is supported by the presence of a small transmitted flux across the He II Ly α spectra at $z \simeq 3.1$ detected by Heap et al. (1999).

Since reionization occurs outside-in and the dense gas can stay neutral until well after the overlap of H II regions, the clumpiness of the IGM does not necessarily increase the mean number of times that a baryon will recombine during the reionization epoch; moreover, this mean number of recombinations does not just depend on the properties of the IGM, but also on the luminosity of the ionizing sources. Thus, for the density distribution suggested by numerical simulations and low-luminosity sources, the number of photons per hydrogen atom required for the reionization is of order unity. In fact, clumpiness can even reduce the required number of photons when a large fraction of baryons are in high density regions that do not need to be ionized in order for the mean free path of the photons to increase to values much larger than the mean separation between sources. Only at very high redshift, when $R_u \gg 1$, recombinations imply a significant increase in the required emissivity for reionization. This modest requirement can be met by both faint QSO's and star-forming galaxies. The remaining uncertainties to determine which sources reionized the IGM are the space density of faint high-redshift QSO's and star-forming galaxies, and the escape fraction of Lyman continuum photons from high-redshift galaxies.

We would like to thank Tom Abel, Piero Madau, and Tom Theuns for helpful discussions. We also thank R. Cen and J. P. Ostriker for giving us permission to show in Figure 1 the density distribution obtained from their numerical simulation. JM thanks the Alfred P. Sloan Foundation for support.

REFERENCES

Abel, T., & Mo, H. J. 1998, ApJ, 494, L151

Anderson, S. F., Hogan, C. J., Williams, B. F., & Carswell, R. F. 1998, AJ, submitted (astr0-ph/9808105)

Arons J., & Wingert D. W. 1972, ApJ, 177, 1

Bahcall, J. N., & Salpeter, E. E 1965, ApJ, 142, 1677

Boksenberg, A., 1997, in Structure and Evolution of the IGM, 13th IAP colloquium, eds. Petitjean P., Charlot S., p. 85

Boksenberg, A., Sargent, W. L. W., & Rauch, M. 1998, to appear in the Proceedings of the Xth Rencontre the Blois, The Birth of Galaxies (astro-ph/9810502)

Boyle B., & Terlevich, R. J., 1998, MNRAS, 293, 49p

Burles, S., & Tytler, D. 1998, ApJ, 507, 732

Cen, R., Miralda-Escudé, J., Ostriker, J. P., & Rauch, M. 1994, ApJ, 437, L9

Davé, R., Hellsten, U., Hernquist, L., Katz, N., & Weinberg, D. H. 1998, ApJ, submitted (astro-ph/9803257)

Davidsen, A. F., Kriss, G. A., & Zheng, W. 1996, Nature, 380, 47

Dey A., Spinrad H., Stern D., Graham J.R., & Chaffee F.H., 1998, ApJ, 498, L93

Dickinson, M. 1998, in STScI Symposium 1997 “The Hubble Deep Field”, eds. M. Livio, S. M. Fall, P. Madau (astro-ph/9802064)

Efstathiou, G. 1992, MNRAS, 256, 43p

Fernández-Soto, A., Lanzetta, K. M., & Yahil, A. 1999, ApJ, 513, 34

Gnedin, N. Y., & Ostriker, J. P. 1997, ApJ, 486, 581

Gruzinov, A., & Hu, W. 1998, ApJ, in press

Gunn, J. E., & Peterson, B. A. 1965, ApJ, 142, 1633

Haardt, F., & Madau, P. 1996, ApJ, 461, 20

Haehnelt, M. G., Natarajan, P., & Rees, M. J. 1998, MNRAS, 300, 817

Haiman, Z., & Loeb, A. 1998, ApJ, submitted (astro-ph/9807070)

Heap, S. R., Williger, G. M., Smette, A., Hubeny, I., Sahu, M., Jenkins, E. B., Tripp, T. M., & Winkler, J. N. 1999, submitted to ApJ (astro-ph/9812429)

Hernquist, L., Katz, N., Weinberg, D. H., & Miralda-Escudé, J. 1996, ApJ, 457, L51

Hogan, C. J., Anderson, S. F., & Rugers, M. H. 1997, AJ, 113, 1495

Hurwitz, M., Jelinski, P., & van Dyke Dixon, W. 1997, ApJ, 481, L31

Jakobsen, P., et al. 1994, Nat, 370, 35

Jakobsen, P. , et. al., 1996, in Benvenuti P. Macchetto F.D., Schreier E.J., “ Science with the Hubble Space Telescope-II, STScI, Baltimore, p. 153

Leitherer, C., Ferguson, H. C., Heckman, T. M., & Lowenthal, J. D. 1995, ApJ, 454, L19

Madau, P., in: Corbelli E., Galli D., Palla F., eds. Molecular Hydrogen in the Early Universe, Mem.S.A., in press, astro-ph/9804280

Madau, P., Haardt, F., & Rees, M. J. 1998, submitted to ApJ (astro-ph/9809058)

Meiksin, A., & Madau, P. 1993, ApJ, 412, 34

Miralda-Escudé J., 1998, ApJ, 501, 15 (M98)

Miralda-Escudé J., Rees M.J., 1994, MNRAS, 266, 343

Miralda-Escudé, J., Cen, R., Ostriker, J. P., Rauch, M., 1996, ApJ, 471, 582

Pei, Y. C. 1995, ApJ, 438, 623

Press, W., Rybicki, G. B., & Schneider, D. P. 1993 ApJ, 414, 64

Rauch, M., Miralda-Escudé, J., Sargent, W. L. W., Barlow, T. A., Weinberg, D. H., Hernquist, H., Katz, N., Cen, R., & Ostriker J. P. 1997, ApJ, 489, 7

Reimers D., Köhler S., Wisotzki L., Groote D., Rodriguez-Pascal P., Wamsteker W., 1997, AA, 327, 890

Scheuer, P., 1965, Nature, 207, 963

Schneider, D. P., Schmidt, M., & Gunn, J. E. 1991, AJ, 102, 837

Shapiro, P., & Giroux, M. 1987, ApJ, 321, L107

Songaila, A., & Cowie, L. L. 1996, AJ, 112, 335

Steidel, C. S., Adelberger, K. L, Giavalisco, M., Dickinson, M., Pettini, M. 1998, ApJ, submitted (astro-ph/9811399)

Storrie-Lombardi, L. J., McMahon, R. G., Irwin, M. J., & Hazard, C. 1994, ApJ, 427, L13

Thoul, A., & Weinberg, D. H. 1996, ApJ, 465, 608

Weymann, R. J., Stern D., Bunker A., Spinrad H., Chafee, F. H., Thompson R. I., & Storrie-Lombardi L. J. 1998, ApJ, 505, L95 (astro-ph/9807208)

Zhang, Y., Meiksin, A., Anninos, P., & Norman, M. L. 1998, ApJ, 495, 63

Zhang, Y., Anninos, P., & Norman, M. L. 1995, ApJ, 453, L57

Zheng, W., Kriss, G. A., Telfer, R. C., Grimes, J. P., & Davidsen, A. F. 1997, ApJ, 492, 855

Zuo L., 1992, MNRAS, 258, 36

Zuo, L., & Phinney, E. S. 1993, ApJ, 418, 28